

## **Chapter 7**

### **7. Elements of optical system**

- 7.1. Passive elements of optical track**
  - 7.1.1. Optical fibers and optical cables**
  - 7.1.2. Splicers and Connectors**
  - 7.1.3. Couplers - splitters**
    - 7.1.3.1. Theoretical principles of directional couplers**
  - 7.1.4. Optical isolators**
- 7.2. Active elements of optical track**
  - 7.2.1. Theoretical background of optical amplifying**
  - 7.2.2. Optical amplifiers**
    - 7.2.2.1. Erbium amplifier EDFA**
    - 7.2.2.2. Raman amplifier**
  - 7.2.3. Semi-conductor amplifier**
  - 7.2.4. Modulators**
    - 7.2.4.1. Pockels and Kerr effects**
    - 7.2.4.2. Mach – Zehnder modulator**
    - 7.2.4.3. Semi-conductor modulator**
  - 7.2.5. Multiplexers and demultiplexers**
  - 7.2.6. Switches**

### **7. Elements of optical system**

The scheme of typical optical track is shown in the Fig. 7.1. Every optical track has to consist of a transmitter, an optical cable and a detector. The optical fibers were described in chapters 1-4. The transmitters are considered in chapter 5, the detectors are discussed in chapter 6.

The first part of the optical track is the transmitter which is the source of light – a LED diode or a laser. The LED diode or the laser are modulated to create PCM signal (pulse-code modulated signal). If the signal is digital, so it represents a sequence of zeros and ones, the simplest coding, called NRZ (non-return-to-zero), is related to the code, in which the lack of light from the light source denotes zero and the presence of light denotes logical one. However, NRZ has many shortages and is often replaced by more effective coding.

The modulated light from a LED diode or a laser enters the fiber through a connector to make the losses of optical power as small as possible. Light propagating through the fiber undergoes optical power reduction, so from time to time it has to be regenerated. It can be enhanced with electronic regenerators or with the help of optical amplifiers. The electronic regenerator is an electronic amplifying device, which change first the optical signal into the electric signal, then amplify it and convert into an optical signal again. The electronic regenerator obviously reduces the speed of data transmission. Therefore, the modern telecommunication systems and computer networks are interested in creating entirely optical nets. In such networks electronic regenerators are replaced by optical amplifiers. Optical amplifiers usually regenerate signal every 50-80 km.

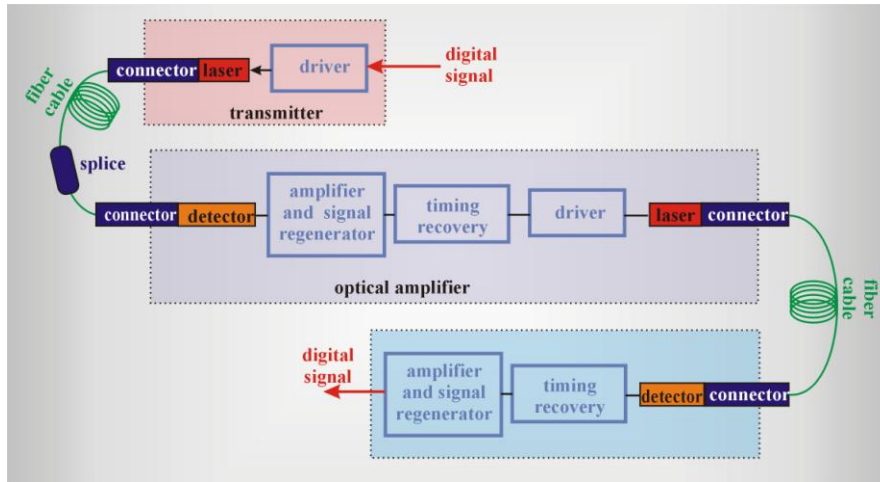


Fig. 7.1 Scheme of the optical track

At the end of the optical track there is always a receiver, which detects optical signal and then converts it into an electric signal, amplifies it and regenerates its shape.

Obviously this simple scheme presented in Figure 7.1 illustrates only idea. The real optical track consists of a great number of elements which will be considered in this chapter:

- optical transmitter which consists of a LED diode or laser and an optical modulator,
- optical fiber optimized in terms of dispersion, non-linearity, attenuation,
- splices and connectors,
- amplifier (erbium amplifier or Raman amplifier),
- optical filters (eg. based on Bragg gratings ),
- isolators,
- couplers and splitters,
- multiplexers and demultiplexers, which are used to add or subtract the channels in WDM system (eg. add/drop multiplexers),
- optical switches,
- electronically controlled optical switches,
- receiver (PIN photodiode and avalanche photodiode),
- electronic elements to signal monitoring and signal processing,
- computers and software used to control of the system operation.

### 7.1.1. Optical fibres and optical cables

Optical fibers and optical cables were discussed in chapters 1 and 2.

### 7.1.2. Splices and connectors

Optical splices and connectors combine two fibers and are one of the most important elements of an optical system. They permit light to pass from one fiber to another. Optical fibers produced in short length distances of 1-2 km have to be connected. The optical connection of two parts of a fiber can be obtained by fusion or mechanical coupling to get the optical coupling of fiber cores so that light can pass. It is not so easy task as fiber connectors must align cores of microscopic sizes. There are two ways that fibers are joined: splices and

connectors. The splices form permanent connections between fibers, enabling construction of long-distance transmission lines between the optical regenerators. The splices are created by fusion or mechanical splicing. To get the fusion splicing the fibers are melted or fused together by heating the fiber ends, usually with an electric arc. The fusion splices provide joints with the lowest loss in the range 0.01 - 0.1 dB for single-mode fibers. The mechanical splicing is an alternative way of making a permanent connection. It is an inexpensive, easy way used particularly in emergency cases for fast restoration. Their losses are higher, typically in the range 0.05 - 0.2 dB for single-mode fibers.

The connectors are not permanent joints and are used in applications where flexibility and fast reconfiguration in routing an optical signal is required as well as in terminating cables.

Termination of optical cables is performed with the connectors called **pigtails**, while to cross optical tracks in telecommunication systems short fiber sections are used – **patch cords** (Fig. 7.2) tipped with suitable connectors.

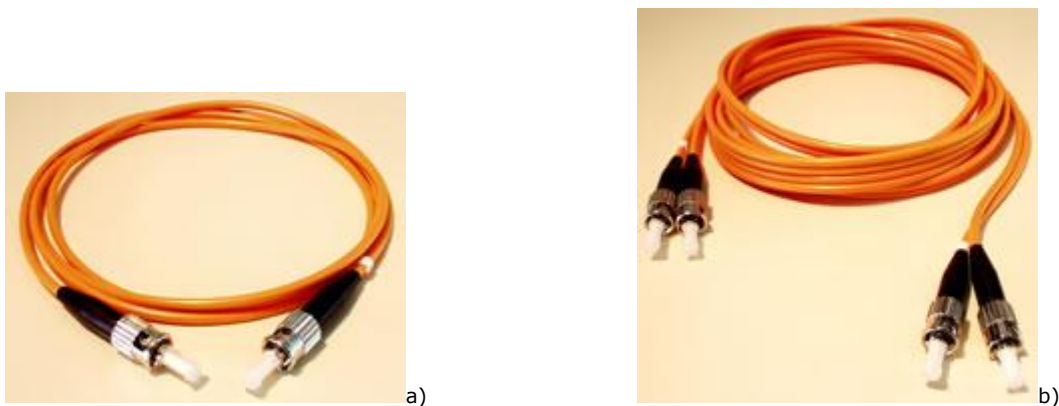


Fig. 7.2 Patch cord, short section of a fiber, terminated with two connectors a) patch cord multimode simplex, ST-ST, b) patch cord multimode ST-ST, duplex <http://www.atel.com.pl>

Losses of connectors are of the order of 0.25-0.5 dB. To get low losses of propagation between the fibers, very precise mechanical positioning of elements is needed to obtain correct coaxial alignment of the fiber cores. There are three main components of the connector design that allow to achieve the proper optical coupling, low losses and full reproducibility: ferrule, connector body and coupling mechanism. Ferrule is a hollowed-out element that actually holds the glass fiber forming a tight grip on one strand of fiber. Ferrules are usually made from ceramic, metal or plastic. The connector body is a plastic or metal structure that holds the ferrule and attaches the connector to the jacket of the fiber cable itself. The coupling mechanism (a latch clip, a bayonet-style nut or similar device) holds the connector in place when it gets attached to another device, for example a switch, bulkhead coupler, etc. Basic requirement in the construction of connectors is reduction of losses, reflections in mechanically and optically stable connection.

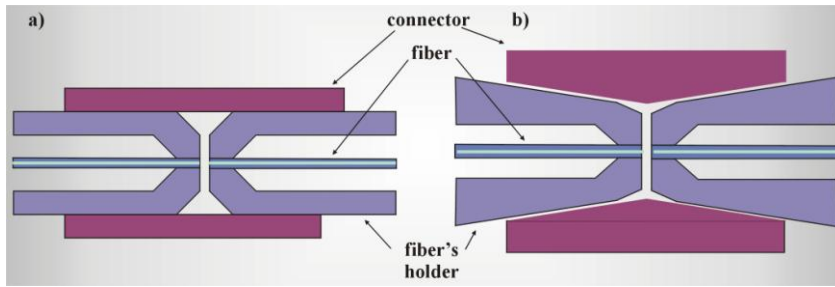


Fig. 7.3 Connectors, a) muff connector , b) cone connector

To get the minimal losses at the connector the precise and repeatable positioning of a core of both optical fibers is very essential. There is a great variety of technologies and standards, just as in copper based cables. Fig. 7.3 presents an example configuration: a muff connector and a cone connector. In the first configuration a fiber is placed in the precise muff (for single-mode optical fibers tolerance is on the order of  $1 \mu m$ ) and then it is stuck and frontally polished. Metal cylinder connects two muffs in which two optical fibers are placed. In the cone connectors, the muff has been replaced by cone shape construction. In the Figure 7.4 the most often used types of connectors for standard glass fibers are presented.

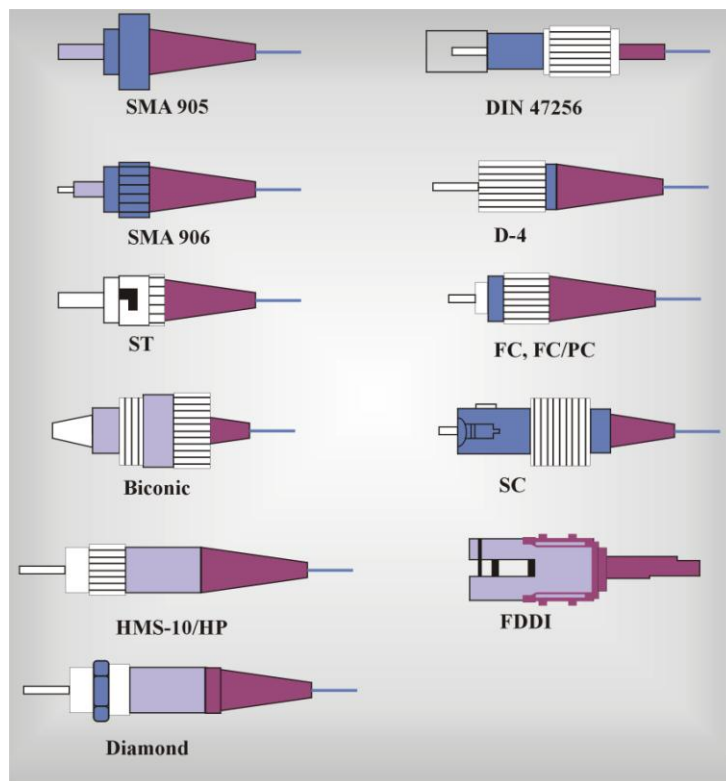


Fig. 7.4 The modern and obsolete standards of connectors for glass fibers

The FC, ST and SC are the most popular and the oldest connectors for many years. The FC is a single mode connector with a 2.5 mm ferrule. It screws on firmly, and exhibits a good performance if you make sure that the key is aligned in the slot properly before tightening. The FC connector has been mostly replaced by SC and ST connectors. The ST connector has a bayonet mount and a long cylindrical 2.5 mm ceramic or polymer ferrule to

hold the fiber. The ST connectors are spring-loaded, so if you have high loss, reconnect them and make sure they are seated properly. The SC type is much more common push-pull connector. It guarantees the improved polarization and mechanical stability. It is also available in a duplex configuration – one for transmission, and second one for receipt (duplex-SC).

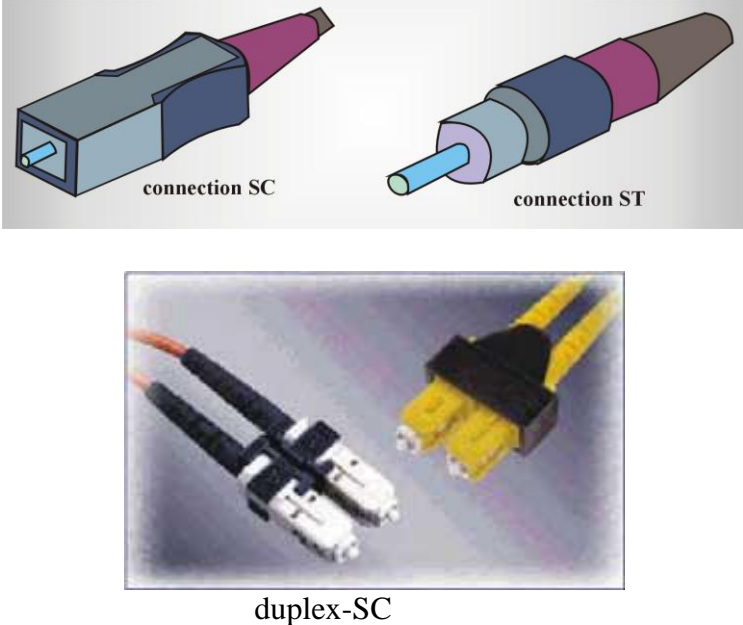


Fig. 7.5 SC, ST and duplex-SC connectors

The another standard of optical connectors is the MT-RJ connector (Figure 7.6) similar to RJ-45 used in copper based cables. MT-RJ connector is a duplex connector with both fibers in a single polymer ferrule, so the transmission channel and the receiving channel cannot be misled, as it can happen when we consider the single connectors ST and SC. It uses pins for alignment and has male and female versions.

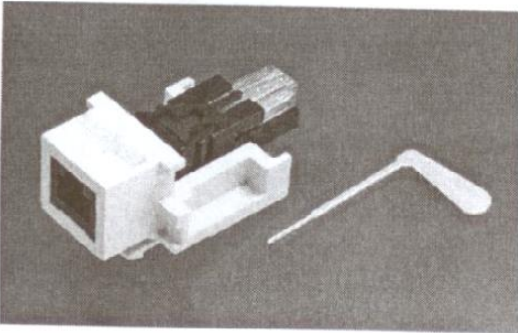


Fig. 7.6 MT-RJ connector

- When choosing the connector we should consider the following factors:
- type of optical fibers which has to be connected, requirements for attenuation limits,
  - environment of the work (aerial installation, building, installing ditches in the ground),

- costs, in case of development or modification of the system backward capability should be considered.

Classification of optical connectors can be considered taking into account the following features:

- type of fibers contact (NC, PC, SPC, APC),
- fibers holding and coupling mechanism,
- technology of configuration (clenches technology, no-glue technology),
- material of which the elements of the connector are made, e.g. connector body and coupling mechanism,
- type of connector (ST, SC, FC, DIN, Bionic SMA).

The different types of contact between fibers and the shape of ferrula forehead are presented in Fig. 7.7. As it was said earlier, ferrula is an element in which fiber is placed. It is used to fix fiber coaxially in its hole. The ferrula can be a part of a fiber connector or of a mechanical connector. For systems with bit rates above 600 Mb/s it is recommended to use angled connectors (APC type). Fig. 7.7 illustrates also another important parameter of connectors, called ORL (optical return loss). This parameter characterizes the loss of light which is reflected from the surface of the connector and returns back to the fiber.

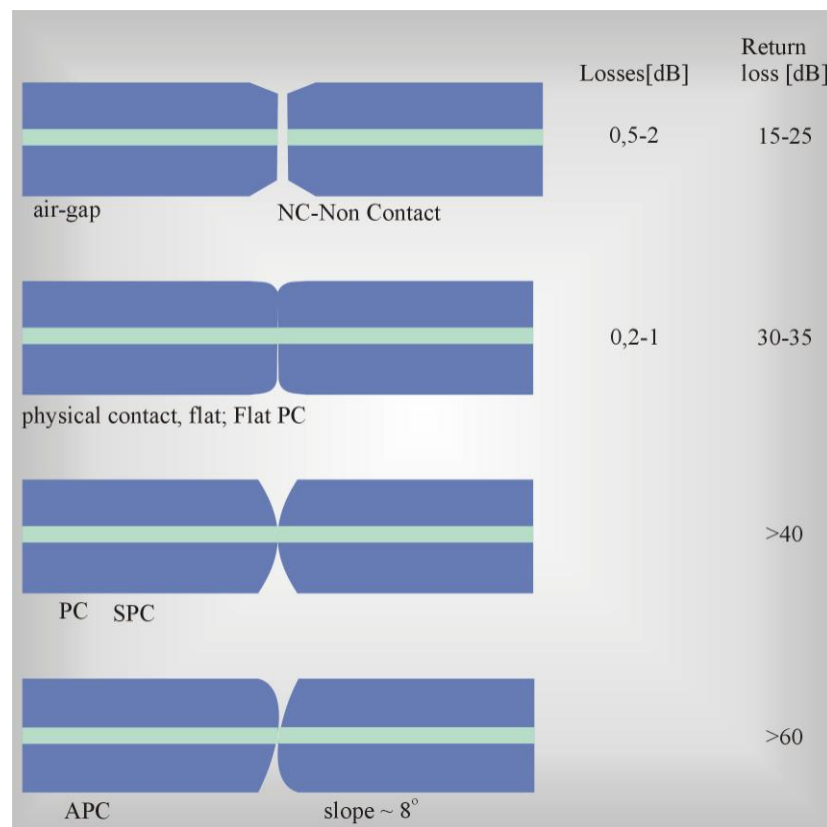




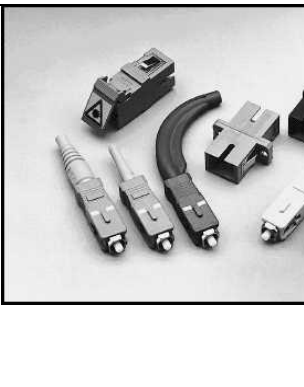
Fig. 7.7 Various types of contact between fibers and the shape of ferrula forehead. Symbols PC - Physical Contact , SPC – Super-polished Physical Contact , it can be also UPC (Ultra-polished Physical Contact ) , AC - Angled Contact ) , the end of fiber is polished under the angle of 8 degrees to plane perpendicular to fiber axis. APC - Angled Physical Contact (angled connection with physical contact)

The classification based on coupling mechanism depends on the way of holding the connector in place when it gets attached to another device. One can distinguish

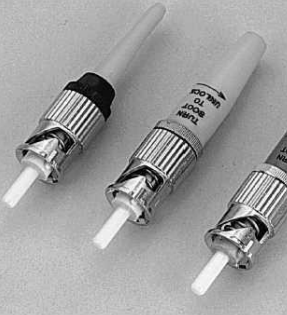

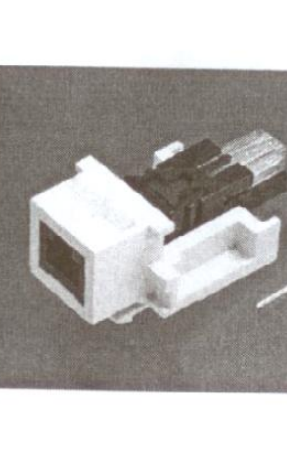
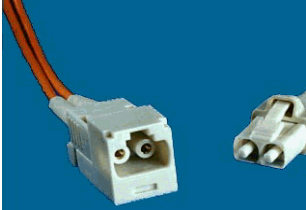
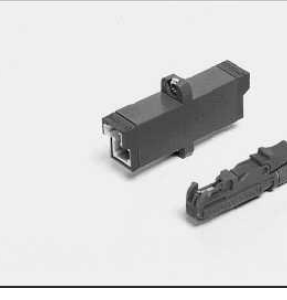
- keyed and non-keyed connectors, called sometimes thumb locked or taper keyed. The thumb locked connectors have their own losses smaller, as it guarantees the same position and relative position of the axes of the connected fibers,
- tuned and non-tuned connectors.

The quality of the connector depends largely on the material of ferrula and a connector body. The ferrula in connectors of high quality is made from zircon ceramics or carbide. The ferrulas of average and low quality are made of polymers, brass, stainless steel. The connector body is made of copper, wolfram carbide, phosphorous bronze, ceramics. Below we will summarize the most popular types of connectors (table 1)

Table 1 Characteristic of most often used types of fiber connectors

	<p>SMA</p>	<ul style="list-style-type: none"> <li>• developed by Amphenol company</li> <li>• one of the first standard for connecting fibers, obsolete standard</li> <li>• still used in some multimode fibers in military and industrial systems</li> <li>• threaded locked joint, non-keyed</li> <li>• non contacting fibers</li> <li>• polished flat surfaces</li> <li>• the newer version of FSMA used in military systems, and older network systems</li> </ul>
	<p>FC (Fiber Connector)</p>	<ul style="list-style-type: none"> <li>• developed by NTT (Japan) as the successor of D3 connector</li> <li>• very good repeatability of parameters</li> <li>• threaded joints</li> <li>• internal spring controls the clamp of fibers</li> <li>• APC version available</li> <li>• mechanical construction assures good mechanical isolation of ferrula and fiber from fixing plate and cable</li> </ul>
	<p>SC (Subscriber Connector)</p>	<ul style="list-style-type: none"> <li>• developed by NTT (Japan)</li> <li>• connector of rectangular section, in the plastic casing; blue for single mode fibers and beige for multimode fibers</li> <li>• thumb locked connection</li> <li>• plastic construction (except of ferrula and blankhold spring)</li> <li>• APC version available for small reflection attenuation applications</li> <li>• standard of ISO and IEC</li> </ul>



		<p>ST (Straight Tip)</p>	<ul style="list-style-type: none"> <li>• developed by AT &amp; T as the successor of Biconic</li> <li>• connector with bayonet mount</li> <li>• the thumb locked joint</li> <li>• ferrula made of polymer, ceramics, phosphorous bronze, copper, wolfram carbide</li> <li>• disadvantage - cheap versions of ST are susceptible to vibrations</li> </ul>
		<p>FDDI</p>	<ul style="list-style-type: none"> <li>• multimode connector</li> <li>• low attenuation, polarization stability</li> <li>• resistance for tensions of the fiber</li> <li>• ceramic ferrulas</li> </ul>
		<p>MT-RJ</p>	<ul style="list-style-type: none"> <li>• duplex connector with both fibers in a single polymer ferrule</li> <li>• imitated on the RJ-45 jack for copper cables</li> <li>• pins for alignment</li> </ul>
 <p><a href="http://www.panduit.com/products/WhitePapers/069414.asp">http://www.panduit.com/products/WhitePapers/069414.asp</a></p>		<p>OPTI-JACK</p>	<ul style="list-style-type: none"> <li>• standard similar to RJ-45</li> <li>• the distance between fibers <math>\frac{1}{4}</math> inch that is twice less than in the duplex SC connector</li> <li>• small sizes allows the miniaturization of ports</li> </ul>
		<p>E-2000</p>	<ul style="list-style-type: none"> <li>• telecommunication, LAN, WAN, CATV, the sensors systems, measurements</li> <li>• integrated landing flap protecting ferrule from the dust</li> <li>• built-in spring guarantees the lock of landing flap.</li> <li>• perfect when the thickness of cross fields is large.</li> </ul>



### 7.1.3. Couplers – splitters

*Optical couplers* are devices, which combine light power from several input fibers into a single fiber or divide optical signals among many output channels. The parameter which characterizes the coupler is  $N \times M$ , where  $N$  the number of input ports and  $M$  is the number of output ports  $M$  (Fig.7.8). Fiber optic couplers attenuate the signal much more than connector or splicer because the input signal is divided among the output ports. For example, in a 1x2 fiber optic coupler, each output power is less than one-half the power of the input signal (over a 3 dB loss).

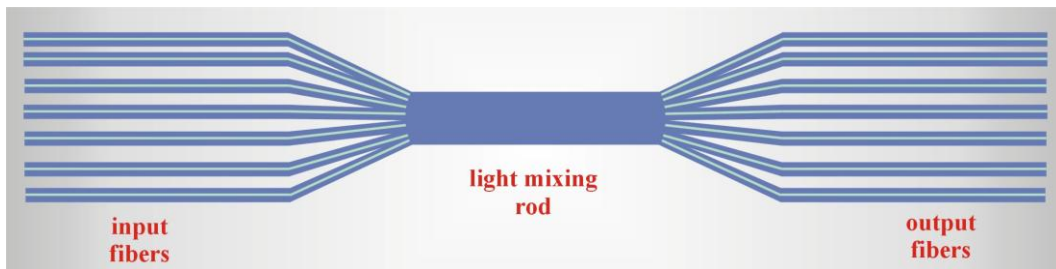


Fig. 7.8 Optical coupler



b)

Fig. 7.9 Illustration of an optical coupler 1x2, single mode 50%:50%, 1310 nm, <http://www.atel.com.pl>

We can divide couplers according to their construction into

- side couplers
- front couplers

We can also divide couplers according to applied technology into

- polished / stuck couplers
- waisting / welded couplers
- optoelectronics integrated technology made couplers

Figures 7.10 and 7.11 present the front coupler and the side coupler.

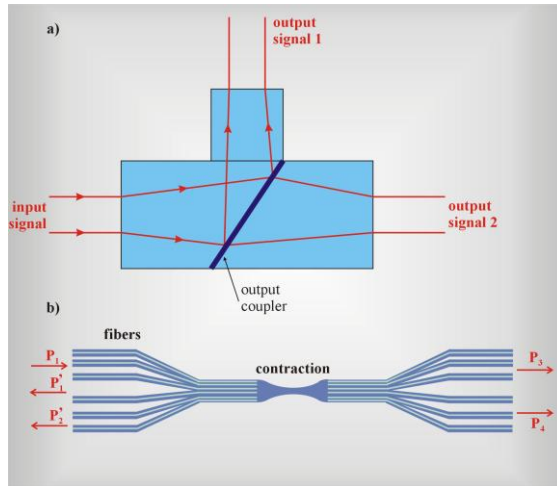


Fig. 7.10 Front coupler (a)

Fig. 7.11 Side coupler (b)

The front coupler employs optical lenses of SELFOC (selffocusing) type (Fig. 7.12) and a semi-transparent mirror. The light which enters the coupler is divided on the mirror into two beams. The mirror transmits part of the light ( $N$ ), and the other part it reflected ( $M$ ) ( $N + M \cong 100\%$ ). This simple configuration forms a 1x2 type coupler. If the mirror is 50%:50%, then the light introduced into the entrance port is divided into the two output ports with identical intensities.

The side coupler of  $N \times N$  type is presented in Fig. 7.11. The couplers of  $N \times N$  type are called star couplers and are used in nets of star topology.

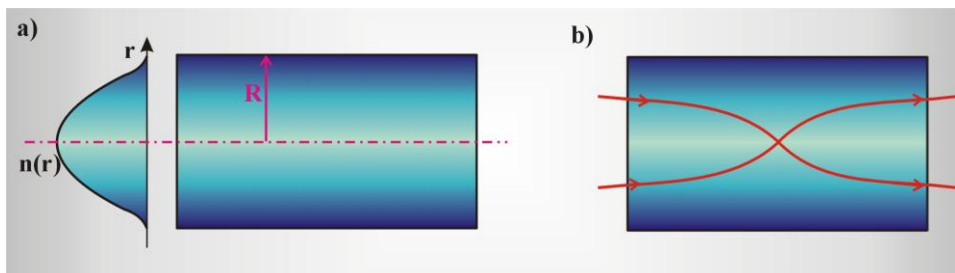


Fig. 7.12 SELFOC type (self - focusing), lens (b) which introduces the light into optical fiber, the profile of refraction index is shown in the left part of the figure (a). The profile of refraction index in material plays the same role in focusing of light as the curvature in traditional convex lenses

The most popular way of production of couplers is twisting and melting together few optical fibers with a burner and stretching until obtaining the desirable power separated between the branches (Fig. 7.13).

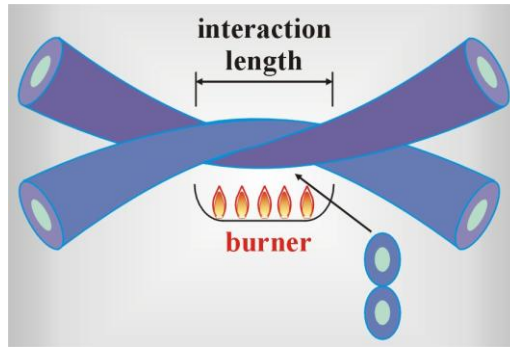


Fig. 7.13 Production of couplers by melting and stretching

Various techniques can be applied to obtain couplers. They can be obtained by polishing and sticking and cut into desirable length to deliver required parameters (Fig. 7.14). However, this method is time consuming, expensive and not suitable for the mass production.

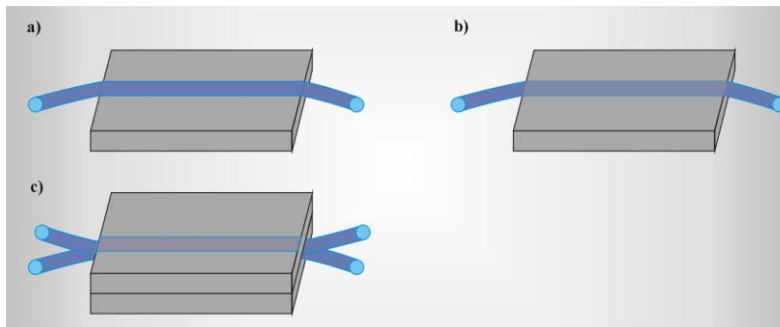


Fig. 7.14 Couplers obtained by polishing and sticking

Couplers can also be produced in the technology of integrated optoelectronics (Fig. 7.15 )

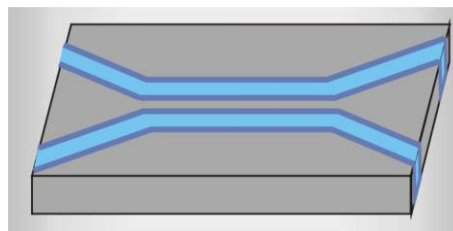


Fig. 7.15 Couplers produced in the technology of integrated optoelectronics

Connecting two fibers and their stretching cause obviously change of propagation conditions and division of power between the coupler branches.

The theoretical description of this phenomena will be presented later in the chapter where we will consider the theoretical fundamentals of couplers. Particularly interesting is the **tunnel optical effect**. Here we will only say that it is possible to modify the parameters of the coupler or the splitter in such way that they become selective. The selective couplers can be sensitive to the wavelength or polarization. The **selective couplers** play very important role in wavelength division multiplexing systems WDM, DWDM, which will be discussed later.

The selectivity of wavelength-sensitive coupler means that division of power depends on the wavelength. So, if we introduce through the entrance port two lengths  $\lambda_1$  and  $\lambda_2$  , in

one of the exit ports will appear only the wavelength  $\lambda_1$ , and in the second one - only  $\lambda_2$  (Fig.7.16).

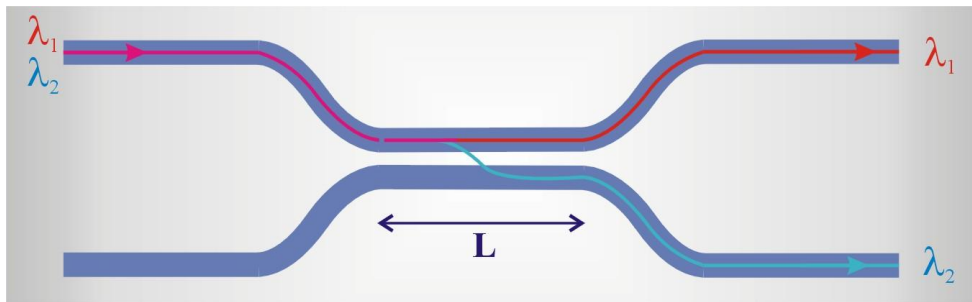


Fig. 7.16 16 Directional coupler employed as the demultiplexer

Therefore, the selective couplers can act as a multiplexer or a demultiplexer in wavelength division multiplexing WDM systems. The manufacturer of couplers defines the ratio of the power division between the input and output branches. For couplers of 1x2 type the most popular ratio of power division of light into output branches are 50%-50%, 90%-10%, 95%-5%, but any power division ratio can be produced on requirement. For example, for the coupler 90%-10% the input power  $100 \mu W$  is divided at the exit ports into  $90 \mu W$  and  $10 \mu W$ . Sometimes this power division is expressed in decibels (dB). The most popular application of optical couplers comprises local computer optical networks LAN. The coupler dimension depends on the network topology. For the star topology ( Fig. 7.17) the star coupler has to be used. If it is the linear bus topology the T type coupler (tee coupler) presented in Fig.7.18 should be employed.

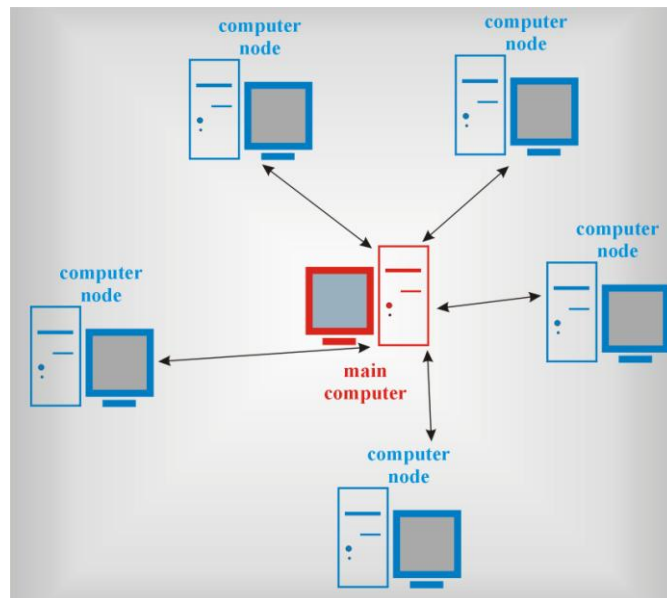


Fig. 7.17 Topology of star in LAN computer network

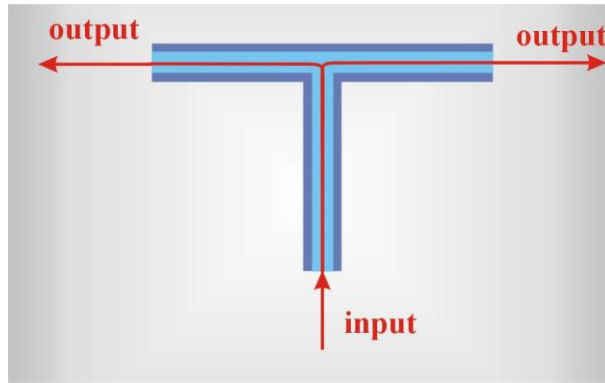


Fig. 7.18 T type coupler employed in linear bus topology

The couplers can be produced as

- planar waveguides
- semi-conductor waveguides
- waveguides based on  $LiNbO_3$  crystals

### 7.1.3.1. Theoretical fundamentals of directional couplers

Let's consider the 2 x 2 coupler, consisting of four ports (Fig. 7.19). Such couplers are called directional couplers. One of the production techniques is side fusing causing that cores of two single-mode fibers are very close to each other. The distances are of the order of the cores diameters and consequently the fundamental modes propagating in single fibers partly overlap in the area of the clad. This partial overlapping leads to optical coupling, which transfers optical power from one core to another when proper conditions are fulfilled.

We distinguish the following couplers

- symmetric, when both cores are identical
- asymmetric, when both cores are not identical

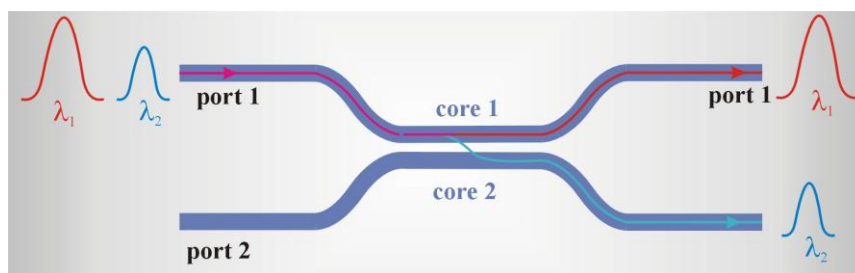


Fig. 7.19 Directional coupler. Schematic illustration of non- linear switching in a coupler. Detailed are explained in the text

In the optical couplers linear and non - linear phenomena take place. We will consider linear phenomena first. To describe exchange of power we will apply theory of coupling modes [1-3]. More details of the theory one might be found in ref.[4].

Let's use the Helmholtz equation

$$\nabla^2 \tilde{E} + \tilde{n}^2(x, y)k_0^2 \tilde{E} = 0 \quad (7.1)$$

describing propagation of light in direction „z” at frequency  $\omega$ , where the wave vector

$$k_0 = \omega / c = 2\pi / \lambda_0 \quad (7.2)$$

describes the propagation in vacuum,  $\tilde{E}(\vec{r}, \omega)$  is the Fourier transform of the electric field  $E(\vec{r}, t)$ , the refraction index  $\tilde{n}(x, y) = n_0$  in the whole area of plane  $(x, y)$ , with exception of the area occupied by the cores of the optical coupler. In this area  $\tilde{n}(x, y) > n_0$ .

Similarly as in chapter 1, where we have described propagation of light in a single fiber we can divide the components in direction „z” - ( $\tilde{A}_z$ ) and in the perpendicular plane  $(x, y)$  - ( $F(x, y)$ ) to write  $\tilde{E}(\vec{r}, \omega)$  as

$$\tilde{E}(\vec{r}, \omega) \approx \hat{e}[\tilde{A}_1(z, \omega)F_1(x, y) + \tilde{A}_2(z, \omega)F_2(x, y)]e^{i\beta z} \quad (7.3)$$

where  $\hat{e}$  is the direction of polarization,  $\beta$  is the propagation constant, indices 1 and 2 denote cores of two approaching fibers. When in the area there is only a single core, the transverse distribution  $F(x, y)$  describe the situation we have considered in chapter 1. Generally the solution for  $F(x, y)$  can be obtained from equation

$$\frac{\partial^2 F_m}{\partial x^2} + \frac{\partial^2 F_m}{\partial y^2} + [n_m^2(x, y)k_0^2 - \beta_m^2]F_m = 0 \quad (7.4)$$

by substituting (7.3) into (7.1) and using the variables separation method.  $\beta_m$  denotes the propagation constant in the fiber 1 or 2 ( $m = 1$  or  $2$ ), and  $n_m(x, y)$  is the refraction index which is  $n_m(x, y) = n_0$  everywhere with exception of the area occupied by the fiber 1 or 2. To find the amplitudes  $A_1$  and  $A_2$  which change along „z” axis of propagating light, we should substitute (7.3) into (7.1), and multiply the equation by the coupled functions  $F_1^*$  and  $F_2^*$ , then use equation (7.4) and integrate over the whole plane  $(x, y)$ . Finally we receive the following equations

$$\frac{d\tilde{A}_1}{dz} = i(\tilde{\beta}_1 + \Delta\beta_1^{NL} - \beta)\tilde{A}_1 + i\kappa_{12}A_2 \quad (7.5)$$

$$\frac{d\tilde{A}_2}{dz} = i(\tilde{\beta}_2 + \Delta\beta_2^{NL} - \beta)\tilde{A}_2 + i\kappa_{21}A_1 \quad (7.6)$$

where  $\kappa_{mn}$  and  $\Delta\beta_m^{NL}$ , ( $m = 1$  or  $2$ ,  $n = 1$  or  $2$ ) describe the degree of the coupling between the fibers in the coupler, and the non-linear term of the propagation constant, respectively. The coupling coefficient of  $\kappa_{mn}$  is given by the formula

$$\kappa_{mn} = \frac{\kappa_0^2}{2\beta} \int \int_{-\infty}^{\infty} (\tilde{n}^2 - n_n^2)F_m^x F_n^x dx dy \quad (7.7)$$

and  $\Delta\beta_m^{NL}$  is expressed by the formula

$$\Delta\beta_m^{NL} = \frac{\kappa_0^2}{2\beta} \int \int_{-\infty}^{\infty} (\tilde{n}^2 - n_L^2)F_m^x F_m^x dx dy \quad (7.8)$$

where  $n_L$  is the linear part of the refraction index  $\tilde{n}$ . In the equations the normalizing condition were applied

$$\int \int_{-\infty}^{\infty} |F_m(x, y)|^2 dx dy = 1 \quad (7.9)$$

Both  $\beta_m$  and  $\kappa_{mn}$  depend on  $\omega$  frequency. Now we will neglect the frequency dependence of  $\kappa_{mn}$  and develop  $\beta_m$  in the Taylor series

$$\tilde{\beta}_m(\omega) = \beta_{0m} + (\omega - \omega_0)\beta_{1m} + \frac{1}{2}(\omega - \omega_0)^2\beta_{2m} + \dots \quad (7.10)$$

The equation (7.5) and (7.6) describing the evolution of amplitudes  $A_1$  and  $A_2$  as a function of length of the coupler are given in the frequency domain. To transform the equations to the time domain we apply the reverse Fourier transformation

$$\frac{\partial A_1}{\partial z} + \beta_{11} \frac{\partial A_1}{\partial t} + \frac{i\beta_{21}}{2} \frac{\partial^2 A_1}{\partial t^2} = i\kappa_{12}A_2 + i\delta_a + (\gamma|A_1|^2 + C_{12}|A_2|^2)A_1 \quad (7.11)$$

$$\frac{\partial A_2}{\partial z} + \beta_{12} \frac{\partial A_2}{\partial t} + i \frac{\beta_{22}}{2} \frac{\partial^2 A_2}{\partial t^2} = i\kappa_{21}A_1 - i\delta_a A_2 + (\gamma_2|A_2|^2 + c_{21}|A_1|^2)A_2 \quad (7.12)$$

We should remember that the second index denotes the number of the fiber, the first one indicates the term in the Taylor development (7.10), so  $(\beta_{1m})^{-1}$  is the group velocity  $v_{gm}$

$$v_{gm} = \frac{1}{\beta_{1m}} \quad (7.13)$$

in the fiber  $m$  ( $m=1$  or  $2$ ). The term  $\beta_{2m}$  describes the effects of group velocity dispersion (GVD) in the fiber  $m$ . Moreover,

$$\delta_a = \frac{1}{2}(\beta_{01} - \beta_{02}) \quad (7.14)$$

$$\beta = \frac{1}{2}(\beta_{01} + \beta_{02}). \quad (7.15)$$

When  $\delta_a = 0$ , both cores of the coupler are identical, so  $\delta_a$  is a measure of the coupler asymmetry. The parameters  $\gamma_m$  and  $c_{mm}$  describe the self phase modulation (SPM), and cross-phase modulation (XPM), which we described in chapter 3. These parameters are expressed by formulas

$$\gamma_m = n_2\kappa_0 \int_{-\infty}^{\infty} \int_{-\infty}^{\infty} |F_m|^4 dx dy \quad (7.16)$$

$$c_{mm} = 2n_2\kappa_0 \int_{-\infty}^{\infty} \int_{-\infty}^{\infty} |F_m|^2 |F_n|^2 dx dy \quad (7.17)$$

When the coupler is symmetric we put

$$\delta_a = 0, \quad \kappa_{12} = \kappa_{21} = \kappa \quad \text{and} \quad c_{12} = c_{21} = \gamma\delta$$

$$v_{g1} = v_{g2} = v_g, \quad \beta_{21} = \beta_{22} = \beta_2$$

and equations (7.11) and (7.12) are simplified to the form

$$\frac{\partial A_1}{\partial z} + \frac{1}{v_g} \frac{\partial A_1}{\partial t} + \frac{i\beta_2}{2} \frac{\partial^2 A_1}{\partial t^2} = i\kappa A_2 + i\gamma(|A_1|^2 + \delta|A|^2)A_1 \quad (7.18)$$

$$\frac{\partial A_2}{\partial z} + \frac{1}{v_g} \frac{\partial A_2}{\partial t} + \frac{i\beta_2}{2} \frac{\partial^2 A_2}{\partial t^2} = i\kappa A_1 + i\gamma(|A_2|^2 + \delta|A_1|^2)A_2 \quad (7.19)$$



Equations (7.11) and (7.12) take simpler form when the continuous wave light (CW) of small power propagates and the non-linear effects and GVD become negligible. Thus, we can put ( $\gamma = c_{12} = \beta_2 = 0$ ) and the time dependence vanishes ( $\frac{\partial A_1}{\partial t} = \frac{\partial A_2}{\partial t} = 0$ ),

$$\frac{\partial A_1}{\partial z} = i\kappa_{12}A_2 + i\delta_a A_1 \quad (7.20a)$$

$$\frac{\partial A_2}{\partial z} = i\kappa_{21}A_1 - i\delta_a A_2 \quad (7.20b)$$

Differentiating (7.20 b) and substituting the result to (7.20 a) we get

$$\frac{d^2 A_1}{dz^2} + \kappa_e^2 A_1 = 0 \quad (7.21)$$

where the coefficient of effective coupling ' $\kappa_e$ ' is defined as

$$\kappa_e = \sqrt{\kappa^2 + \delta_a^2} \quad \kappa = \sqrt{\kappa_{12}\kappa_{21}} \quad (7.22)$$

Doing the same way for  $A_2$  we get the same type of equation.

Presented in Fig.7.19 coupler works in such way that the light is introduced through the port 1, so  $A_1(0) = A_0$ ,  $A_2(0) = 0$ . Using these boundary conditions the equations (7.20 a) and (7.20 b) can be easily solved giving the following expressions

$$A_1(z) = A_0 [\cos(\kappa_e z) + i(\delta_a / \kappa_e) \sin(\kappa_e z)] \quad (7.23)$$

$$A_2(z) = A_0 (i\kappa_{21} / \kappa_e) \sin(\kappa_e z)$$

These equations illustrate the work of the directional coupler. We can see that although we don't introduce the light into the port 2 ( $A_2(0) = 0$ ), it appears in the exit port 2 ( $A_2(z) \neq 0$ ). The intensity of the light in the output port 2 depends on the ratio of the coupling coefficients  $\kappa_{21} / \kappa_e$  (while  $\kappa_e$  depends on the coefficient of asymmetry  $\delta_a$ ) and on the coupler length  $L = z$ . The maximum of power transferred to port 2 is achieved at  $\kappa_e z = m\pi / 2$ , where m is the integer. The term  $L_c = \frac{\pi}{2\kappa_e}$  (at m = 1) is called the coupler length.

Fig. 7.19a presents a power fraction transferred to the second core (port 2)  $\left| \frac{A_2}{A_0} \right|^2$  as function of the coupler length z for several values of  $\frac{\delta_a}{\kappa}$ .

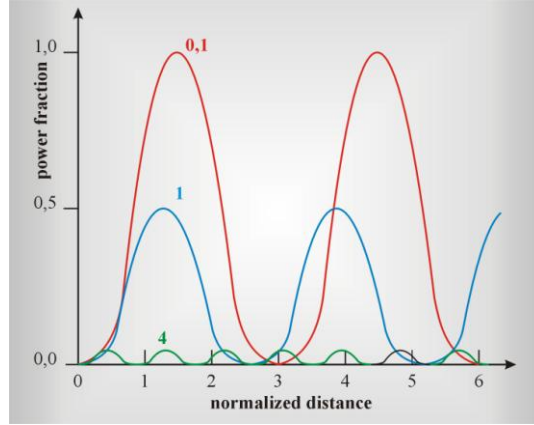


Fig. 7.19a Power fraction transferred to the second core ( port 2 in Fig. 7.19 )  $\left| \frac{A_2}{A_0} \right|^2$  as

a function of the coupler length  $z$  for several different values of  $\frac{\delta_a}{\kappa}$ .

For a symmetric coupler ( $\delta_a = 0, \kappa_e = \kappa$ ) of length  $L$  the equations ( 7.23) take the form

$$A_1(L) = A_0 \cos(\kappa L) \quad (7.24)$$

$$A_2(L) = A_0 \sin(\kappa L)$$

and the distribution of power  $P$  are expressed with the formulas

$$P_1(L) = P_0 \cos^2(\kappa L) \quad (7.25)$$

$$P_2(L) = P_0 \sin^2(\kappa L)$$

where  $P_0 = A_0^2$ .

When the coupling coefficient and length  $L$  of the coupler are chosen in such a way that  $\kappa L = \pi / 4$  we get

$$\frac{P_1(L)}{P_2(L)} = 1 \quad (7.26)$$

which indicates that the power is divided equally ( 50÷50coupler or 3dB). Changing the length of the coupler and distance between the cores of the coupler fibers one can produce the coupler of various division ratios. The coupling coefficient can be determined from the formula (7.7). In practice the following formula applies to estimate the coupling coefficient [5]

$$\kappa = \frac{\pi V}{2\kappa_0 n_0 a^2} \exp[-(c_0 + c_1 \bar{d} + c_2 \bar{d}^2)] \quad (7.27)$$

where  $V$  is so called the normalized cut-off frequency (considered in chapter 1) given by the formula  $V = \kappa_0 a (n_1^2 - n_2^2)^{\frac{1}{2}}$ , where  $a$  is fiber diameter,  $\bar{d} = \frac{d}{a}$  is a normalized distance between the cores of a coupler,  $c_0, c_1, c_2$  are some parameters dependent on  $V$

$$c_0 = 5,2789 - 3,663V + 0,3841V^2$$

$$c_1 = -0,7769 + 1,2252V - 0,0152V^2$$

$$c_2 = -0.0175 + 0.0064V - 0.0009V^2$$

Equations (7.23) and (7.25) illustrate that the coupler exchanges power periodically between two cores. This property of the couplers is employed in optic fiber technology in optical switches .

When instead of continuous wave (CW) we consider a pulse of light propagating in a fiber, we should take into account the effects of the group velocity dispersion (GVD), even if the energy of an optical pulse is small and non - linear effects are neglected.

Equations (7.18 ) can be written in the form

$$\frac{\partial A_1}{\partial z} + \frac{i\beta_2}{2} \frac{\partial^2 A_1}{\partial T^2} = i\kappa A_2 \quad (7.28)$$

$$\frac{\partial A_2}{\partial z} + \frac{i\beta_2}{2} \frac{\partial^2 A_2}{\partial T^2} = i\kappa A_1$$

where  $T = t - \frac{z}{v_g}$ .

We should remember from chapter 3 that the GVD effects are neglected when the length of a fiber  $L \ll L_D$ , where

$$L_D = \frac{T_0^2}{|\beta_2|} \quad (7.29),$$

and the term of  $T_0$  is related to the pulse duration. Because in practice  $L \approx L_c = \frac{\pi}{2\kappa_e}$ ,

where  $L_c$  is the length of the coupling, so GVD is neglected in couplers for which the following condition is fulfilled

$$\kappa L_D \gg 1 \quad (7.30)$$

It is easy to estimate that GVD effects are important only for ultra-short pulses  $T_0 \leq 0.1 ps$ . For pulses longer than 0.1 ps the typical lengths are  $L_c < 1 m$ ,  $L_D > 1 km$  and the coupler behaves identically as for the continuous waves, exchanging periodically the power between the cores of the fibers. Moreover, during the exchange the temporary shape of the pulse is kept constant as long as we can neglect the frequency  $\omega$  dependence of the coupling coefficient  $\kappa$ .

If it is not possible to neglect  $\kappa_1$  and  $\kappa_2$

$$\kappa(\omega) \approx \kappa_0 + (\omega - \omega_0)\kappa_1 + \frac{1}{2} (\omega - \omega_0)^2 \kappa_2 \quad (7.31)$$

then equations (7.28) take the form

$$\frac{\partial A_1}{\partial z} + \kappa_1 \frac{\partial A_2}{\partial T} + \frac{i\beta_2}{2} \frac{\partial^2 A_1}{\partial T^2} + \frac{i\kappa_2}{2} \frac{\partial^2 A_2}{\partial T^2} = \frac{\partial A_2}{\partial z} + \kappa_1 \frac{\partial A_1}{\partial T} + \frac{i\beta_2}{2} \frac{\partial^2 A_2}{\partial T^2} + \frac{i\kappa_2}{2} \frac{\partial^2 A_1}{\partial T^2} = i\kappa_0 A_1 \quad (7.32)$$

When we neglect the non - linear term ( $\kappa_2 = 0$ ) and GVD term ( $\beta_2 = 0$ ) we get

$$A_1(z, T) = \frac{1}{2} \left[ A_0(T - \kappa_1 z) e^{i\kappa_0 z} + A_0(T + \kappa_2 z) e^{-i\kappa_0 z} \right] \quad (7.33)$$

$$A_2(z, T) = \frac{1}{2} \left[ A_0(T - \kappa_1 z) e^{i\kappa_0 z} - A_0(T + \kappa_1 z) e^{-i\kappa_0 z} \right] \quad (7.34)$$

where  $A_0(T)$  is the temporary pulse at  $z = 0$ .

One can see from the equation (7.34) that the pulse  $A_0(T)$  does not keep its shape any longer during propagation through the coupler and undergoes the splitting into two pulses. This effect is called the intramode dispersion. This phenomenon reminds birefringence which can be observed in optical fibers as a result of polarization dispersion. Polarization dispersion has been considered in chapter 1.

Until now we considered couplers of small power in which the non - linear effects can be neglected. However, properties of couplers undergo dramatic changes when we apply higher powers. These properties depend on non - linear effects and play important part in optical switches. Later we will explain why the nonlinearity influences the coupler so strongly. Now we will show only that it is nonlinearity that causes that the output power in ports 1 and 2 depends on the input power  $P_0$  in the way introduced schematically in Fig. 7.20.

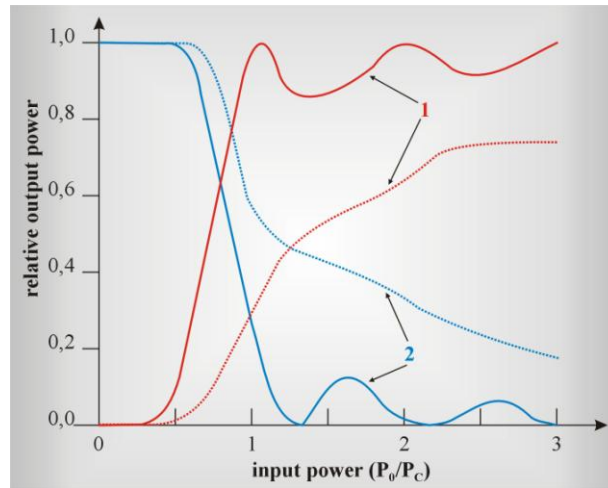


Fig. 7.20 Output power in the non-linear directional coupler for  $\kappa L = \frac{\pi}{2}$

One can see from Fig. 7.20 that at powers smaller than the critical value  $P_c$  almost 100% of power is transferred by the exit port 1. Further increase of the power above  $P_c$  leads to the dramatic reduction of the power in the port 1, while the power passing through port 2 increase dramatically almost to 100%. Therefore, controlling the input power, one can steer the work of the exit ports, by switching power from the port 1 to the port 2 and inversely. The coupler acts as a switch using non - linear effects.

Let us simplify the conditions and assume that the coupler is symmetrical, propagates continuous wave and the GVD effects can be neglected. Thus, the equation (7.18) gets the form

$$\frac{dA_1}{dz} = i\kappa A_2 + i\gamma \left( |A_1|^2 + \delta |A_2|^2 \right) A_1 \quad (7.35)$$

$$\frac{dA_2}{dz} = i\kappa A_1 + i\gamma(|A_2|^2 + \delta|A_1|^2)A_2$$

Equations (7.35) can also be used in quasi – continuous wave approximation, for pulses satisfying the condition

$$L_D \gg L \quad (7.36)$$

where  $L_D$  is the dispersion length,  $L$  is the coupler length.

Expressing the intensity ( $j = 1,2$ ) of the field in  $z$  direction by the power  $P_j$  and phases  $\phi_j$  ;

$$A_j = \sqrt{P_j} \exp(i\phi_j) \quad (7.37)$$

Substituting (7.37) to (7.35) we get

$$\begin{aligned} \frac{dP_1}{dz} &= 2\kappa\sqrt{P_1P_2} \sin \phi \\ \frac{dP_2}{dz} &= -2\kappa\sqrt{P_1P_2} \sin \phi \\ \frac{d\phi}{dz} &= \frac{P_2 - P_1}{\sqrt{P_1P_2}} \kappa \cos \phi + \frac{4\kappa}{P_c} (P_2 - P_1) \end{aligned} \quad (7.38)$$

where  $P_c$  is a critical power

$$P_c = 4\kappa / [\gamma(1 - \delta)] \quad (7.39)$$

where  $\phi = \phi_1 - \phi_2$  denotes the difference of phases between two cores of the coupler.

Because we assumed that the coupler is symmetrical, the difference of phases can be generated only via the non - linear effects as both cores are identical. Indeed, only the effects of self-phase modulation (SPM) and crossing phase modulation (XPM) ( $\gamma \neq 0$ ) can explain, why in identical fibers of the coupler the difference of phases is occurring. The optical powers in both cores of the coupler are different, and SMP and XPM effects which depend on power, generate different phases in both cores.

It has been shown [6] that the solutions to equations (7.38) are given by the expressions

$$\begin{aligned} P_1(z) &= |A_1(z)|^2 = \frac{1}{2} P_0 [1 + \text{cn}(2\kappa_2 z / m)] \\ P_2(z) &= P_0 - P_1(z) \end{aligned} \quad (7.40)$$

where  $\text{cn}(x/m)$  is the elliptic Jacobi function, where  $m = (P_0 / P_c)^2$  .

The dependence of power on the coupler length described by (7.40) is illustrated in Fig. 7.22. We can distinguish the following cases

- when  $m \ll 1$ ,  $P_0 \ll P_c$  then  $P_1(z) = P_0 \cos^2(\kappa z)$ . This case corresponds to small powers and is described by equation (7.25) what is adequate to situation of periodical transfer of power between cores as a function of length  $z$  in the coupler.

- when  $m = 1$ ,  $P_0 = P_c$  then  $P_1(z) = \frac{1}{2} P_0 (1 + \text{sec}(2\kappa z))$ , 50% of power of

one core is transferred to the second one, independently of the coupler length.

• when  $m \gg 1$ ,  $P_0 \gg P_c$ . This case corresponds to large optical powers. The solution is also periodical, as in the first case, but the power is almost entirely transferred to the second core.  $P_2(z) = P_0 \cos^2(\kappa z)$ , and a power in core 1 is reduced almost to zero.

Until now we focused on symmetric couplers mainly for simplifying the theoretical considerations. However, the asymmetric couplers play an important role in optical telecommunication as the WDM filters (add - drop WDM Filters). The asymmetry can be assured by different shape or length of coupler cores. The other way is using the Bragg grating, which we considered in chapter 5. Fig. 7.21 presents the scheme of the grating-assisted fiber coupler.

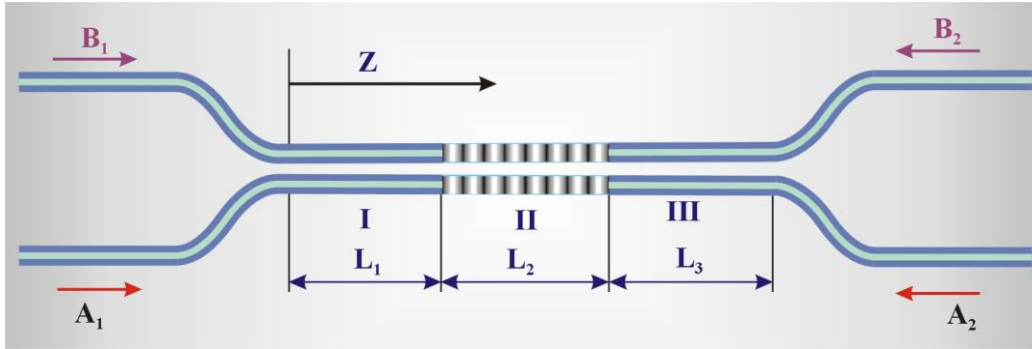


Fig. 7.21 Scheme of grating-assisted fiber coupler.

In practice we use different versions of scheme given in Fig. 7.21 eg.:

- Bragg grating only in one core
- Bragg grating in both cores.

Fundamentals of producing the Bragg grating in fibers were discussed in chapter 5. In planar waveguides the simplest way to generate the Bragg grating is periodic change of thickness of one of waveguides in a coupler. The change of thickness causes the modulation of the coupling coefficient " $\kappa$ ". The grating constant is chosen in a such way that the propagation constants  $\beta_1$  and  $\beta_2$  of cores fulfill the condition

$$\bar{\beta}_1 - \bar{\beta}_2 = \beta_g = \frac{2\pi}{\Lambda} \quad (7.41)$$

In case of the cylindrical couplers, the Bragg grating is created by modulation of the refraction index of the core which is practically achieved by methods discussed in chapter 5.

Let us consider, how the application of Bragg grating in the couplers permits to use them as add/drop filters WDM. Let the Bragg grating to be produced only in one core and the grating constant corresponds to fulfill the condition of reflection for the wave  $\lambda_1$ . If the multichannel signal WDM ( $\lambda_1, \lambda_2, \lambda_3, \dots$ ) is introduced by the entrance port 1 to the core without the Bragg grating, the transfer of power to the second core where Bragg grating is take place for all wavelengths as a result of coupling. All lengths except of  $\lambda_1$ , propagate to the exit port 2, whereas the wave  $\lambda_1$  is reflected and appears in the entrance port 2. In such configuration the coupler acts as filter of "drop" type. However, it can also act as filter of "add" type. Indeed, when we introduce the signal  $\lambda_1$  by the exit port 1 without gratings, it will appear in the exit port 2 as a result of power transfer to the second core and then the reflection from the Bragg grating.

### 7.1.4. Optical isolators

Optical isolators are used in laser technologies for many years. They prevent returning of the light beam emitted by laser back to the resonator cavity. This phenomenon is extremely unfavorable for lasers working in mode locking regime and amplifiers. Therefore isolators are placed in fiber tracks to protect sensitive devices. They are often integrated with laser in laser module and protect light source from back scattered light. We distinguish polarization-dependent and polarization-independent isolators. The polarization-dependent isolators transmit light polarized only in one specific direction. The polarization-dependent isolators are used in optical transmission, cable television, coherent transmission to block reflected and scattered signals. The polarization-independent isolators transmit the light polarized in all directions and can be used in optical amplifiers. The polarization-independent isolators are characterized by small dispersion dependence on polarization and they are used in telecommunication systems of high bit rates, optical amplifiers, as well as in the cable television.

The optical isolator consists of a Faraday rotator and polarizing elements. The Faraday rotator consists of a crystal which is placed in the magnetic field. The Faraday rotator changes the angle of polarization plane of the transmitted light (Fig. 7.22). The change of polarization results from the Faraday effect, one of the well-known magneto-optic effects. When a magnetic field is applied, the optical axis of the material (crystal) becomes twisted.

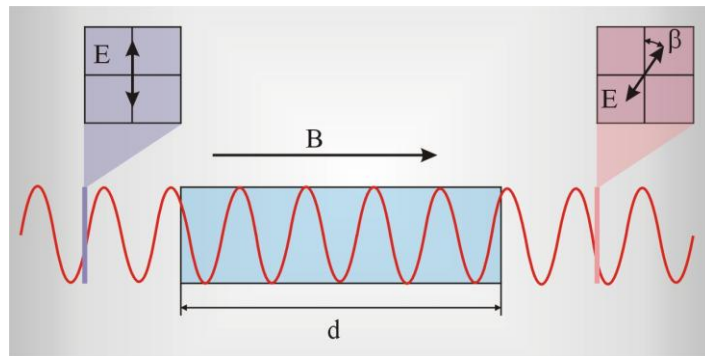


Fig. 7.22 Illustration of polarization plane twisting in Faraday rotator

The rotation angle is expressed by formula

$$\beta = \nu B d$$

where  $\beta$  is the rotation angle (in radians),  $\nu$  is the Verdet constant (radian / (tesla \* m)  $B$  is the intensity of the magnetic field (in tesla),  $d$  is the length (expressed in meters) of optical path on which light interacts with the magnetic field  $B$  in material. The twisting of the polarization plane can be explained as follows. Linearly polarized input light can be presented as combination of two components polarized circularly in opposite directions (right-handed and left-handed circular polarization) (Fig. 7.23)



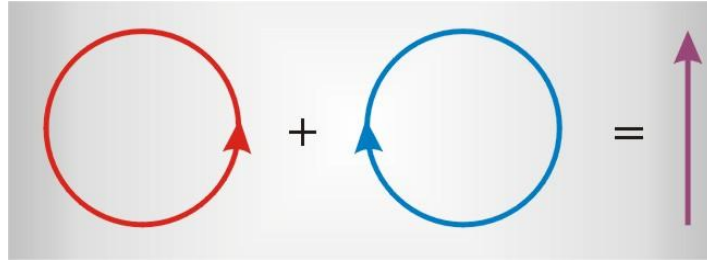


Fig. 7.23 Illustration of light polarized linearly as the result of two component polarized circularly in opposite directions

If we imagine electrons of atoms of material which are moving on orbits, the part of them will rotate in the same direction as the circular polarization vector, and the rest - in the opposite direction. The movement of electrons is related to the refraction index. When the external magnetic field is applied, the change of refraction index takes place (because the movement of electrons undergoes the change under the Lorentz force  $F = qvB$ ). Both right and left polarized components "feel" the change of the refraction index, but each component responds in different way. In consequence, the beam of light divides into two circularly polarized beams propagating with different velocities. This phenomenon is called the Faraday effect or circular birefringence (in analogy to ordinary and extraordinary ray, which propagate through material with different velocities). The different velocity causes the phase difference between the rays which increases with length of optical path. The beam polarized circularly in the same direction as the movements of electrons undergoes the influence of electrons and the direction of polarization twists, while the beam with the vector of the electric field in the opposite direction - not. It should be emphasized that for light reflected back to Faraday rotator does not undergo reverse polarization twisting and does not undergo canceling effect of polarization change in case of backward light. This property results in the fact that Faraday rotator combined with polarizers acts as isolator for light reflected back in the fiber.

The materials used as Faraday rotators are mostly the ferromagnetic materials, such as crystal of YIG ( $Y_3Fe_5O_{12}$ ), as well as  $(TbBi)_3(FeAl)_5O_{12}$  or YIG ( $Y_3Fe_5O_{12}$ ). Another group of materials that also changes polarization exhibit *optical activity*. Many biological structures, with helical symmetry and some inorganic substances – selenium, quartz, tellurium exhibit such properties.

The optical isolator consists of Faraday rotator and two polarizing elements (Fig. 7.24).

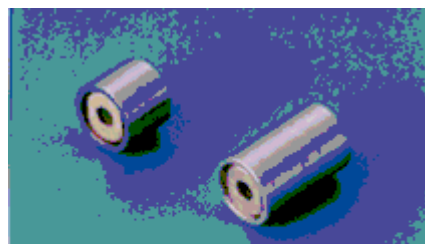
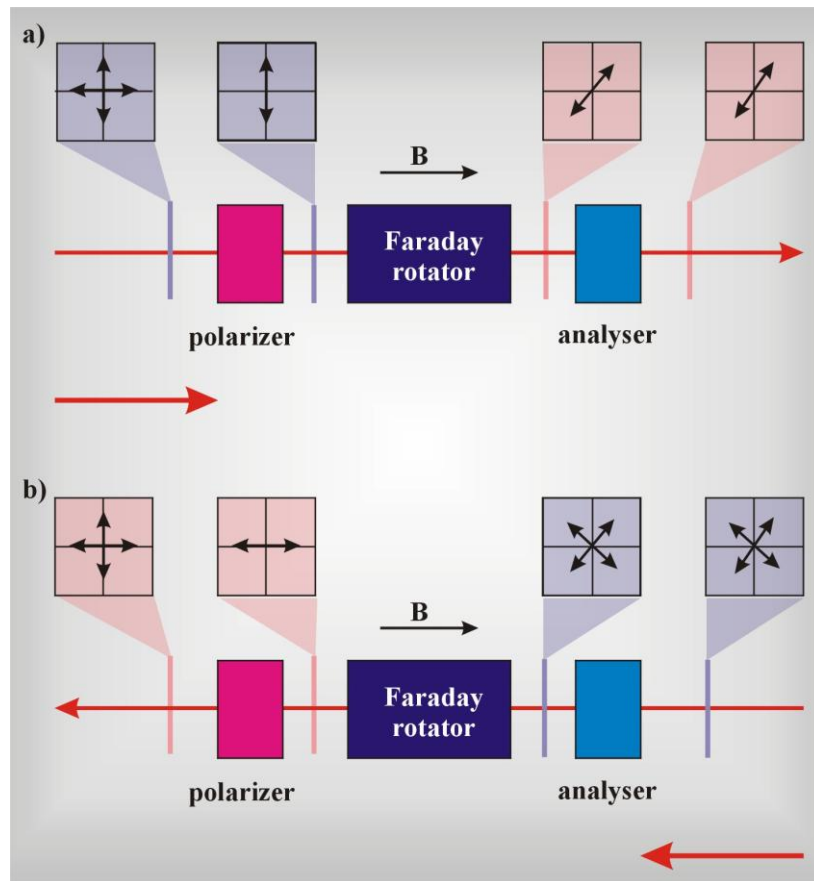


Fig 2 Photograph of polarization dependent optical isolators.

Fig. 7.24 Polarization dependent optical isolator

The first polarizing element in Fig. 7.24 plays a role of a polarizer, the second one - a polarization analyzer. Their optical axes are turned by the angle of  $45^\circ$ . Non-polarized light going through the polarizer becomes polarized light after the first polarizer. In Faraday rotator the plane of its polarization is turned over the angle of  $45^\circ$  and it goes through polarization analyzer. This arrangement acts in a completely different way for light coming from the opposite direction. The backward light (non-polarized) becomes polarized at angle of  $45^\circ$  passing through the analyzer, then going through Faraday rotator the polarization rotates further by  $45^\circ$  in the same direction. It has now polarization turned over  $90^\circ$  with respect to the optical axis of the entrance polarizer and in consequence the backward light does not pass through entrance polarizer. Typical sizes of isolators are 3-5 mm x 3-5 mm, typical losses - 0.2 dB for the forward beam and 40 dB - for the backward beam.

Fig. 7.25 presents the polarization dependent optical isolator. Optical isolator consists of Faraday rotator and two polarizing elements. In this case however, they are not as it was

previously the polarizer and polarization analyzer, but birefringent plates, usually made from crystal layer of  $\text{TiO}_2$ .

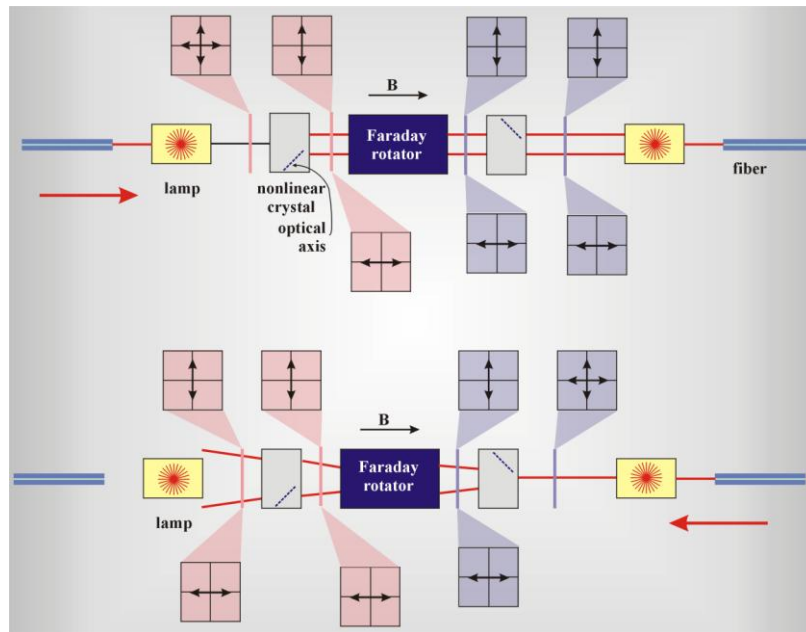


Fig.4 Photograph of polarization independent optical isolators.

<http://www.atel-fiberoptic.com.pl/ie/produkty/pdf/M.pdf>

Fig. 7.25 Polarization independent optical isolator

The entrance birefringent plate causes that the beam of light is separated into ordinary ray and extraordinary ray. Then the polarization plane of each of the rays rotates by  $45^\circ$  passing through the Faraday rotator and then through the second birefringent plate which has the optical axis turned by  $45^\circ$  with respect to the first plate. As a consequence, both rays do not change their properties. On the other hand, the backward light behaves completely different. The backward light passing the birefringent plate No.2 is divided into the ordinary and the extraordinary rays (along the optical axis of the plate). Then both rays turn their polarization by  $45^\circ$  and they enter the plate No.1. However, now the ray, which was extraordinary in plate No. 2 becomes ordinary ray for plate No. 1, while the ordinary one changes into the extraordinary. As a consequence, the rays passing through the plate No.1 are not parallel to each other, so they cannot enter into the optical fiber. At the ends of the isolator there are lenses, which introduce light into fiber. Typical losses of the polarization independent isolators are 0.2 dB for the forward beam, 40 dB for the isolation efficiency of the incident and the backward beam, 60 dB – for the backward beam.

On the other hand, a backward light incident on the same optical isolator is separated into ordinary and extraordinary rays whose relation is reversed with that of a forward light

due to the non-reciprocity of the Faraday rotation. Consequently, rays passing through the No.1 birefringent plate do not become parallel to each other, so they cannot be converged into the upstream optical fiber.

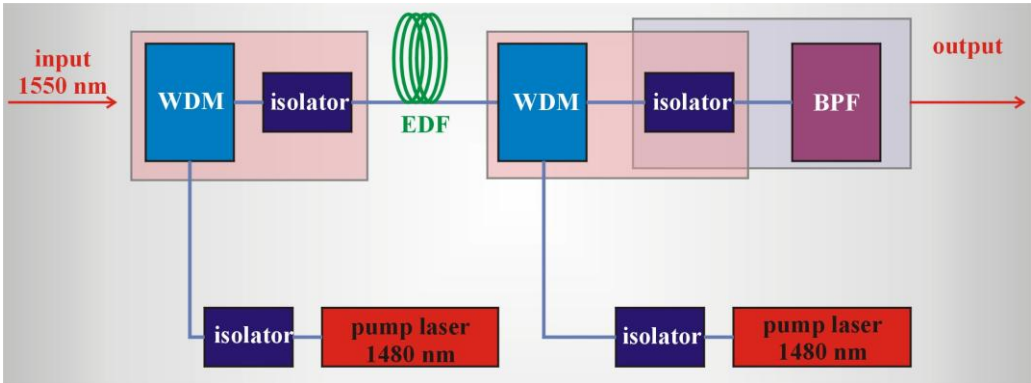


Fig. 7.26 Optical isolators in WDM system

Figure 7.26 presents the typical application of optical isolators in WDM system with erbium amplifier. We can notice that isolators are placed before the pumping lasers and before the erbium amplifier. Fig. 7.26 describes the situation when amplifier is pumped from both sides. When we apply configuration with forward pumping or backward pumping isolators are not needed.

Fig. 7.27 presents the optical isolator applied in forward pumping. The typical sizes are 25 x 30 x 8 mm, losses are on the order of 0.8 dB at 1550 nm and at pumping light of 1480 nm, isolation on the order of 40 dB, reflection attenuation of about 55dB.

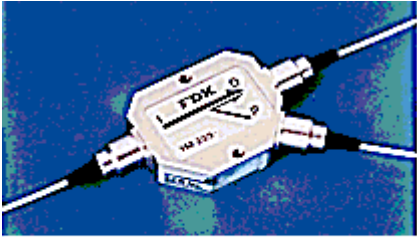


Fig.6 Photograph of optical isolator module.

Fig. 7.27 Photograph of optical isolator module

### 7.2. Active parts of optical track

Light traveling in an optical fiber undergoes attenuation. For short distances the attenuation can be neglected. When the optical signal must be sent on large distances, the attenuation begins to play an important role and the signal has to be regenerated. In high bit rate transmission systems the traditional electronic regenerators are replaced with optical amplifiers of EDFA (erbium doped fiber amplifier) which work in the transmission window of 1.5-1.6  $\mu\text{m}$ . The system of optical amplifiers, known as TAT -12 system, is used in transatlantic transmission between United States, France and England.

Obviously, for these advantages of optical amplifiers some price should be paid. Transmission on large distances causes that the phenomena of dispersion, polarization effects,

ASE (amplified stimulated emission) and non - linear phenomena, which can be neglected in traditional systems, start to cause serious problems. Firstly we will explain the principle of optical amplification generally and then we will apply this theoretical background to explain the optical amplification in erbium doped amplifiers EDFA , Raman amplifiers and in semi-conductive amplifiers.

### 7.2.1. Theoretical fundamentals of amplification [5]

Output pulse energies from femtosecond lasers typically do not exceed a few nanojoules, and peak powers of megawatts. For many applications, higher energies or peak powers are required. Researchers are seeking methods to shorten pulses, to increase peak powers and peak intensities on targets. Given the limits on further trimming of the pulse duration, further increases in peak power and peak intensities can only be obtained by increasing output energy. Amplification of energy from the femtosecond lasers makes possible terawatt peak powers. Amplification, combined together with the initial pulse stretching and compression as a final stage can convert terawatt systems into petawatt lasers with subpicosecond pulses.

So far the highest energies, peak powers and irradiance can be achieved in Nd:glass amplifiers, not those based on Ti:sapphire. The most powerful laser in the world (in 2003) is “Vulcan” in Rutherford Appleton Laboratory, United Kingdom delivering 2.5 kJ in two 150 nm beams, 1 pW,  $10^{21}$  W/cm<sup>2</sup> and Nova system at Lawrence Livermore National Laboratory delivering 1.3 kJ pulse at 800 ps that can be compressed to 430 fs to achieve 1.3 pW and  $10^{21}$ W/cm<sup>2</sup>.

When a laser pulse passes through an optically active material in which the population inversion is maintained by a pumping source, it gains energy from the stimulated emission generated by itself in the medium. As a result the output pulse is amplified (fig. 7.28).

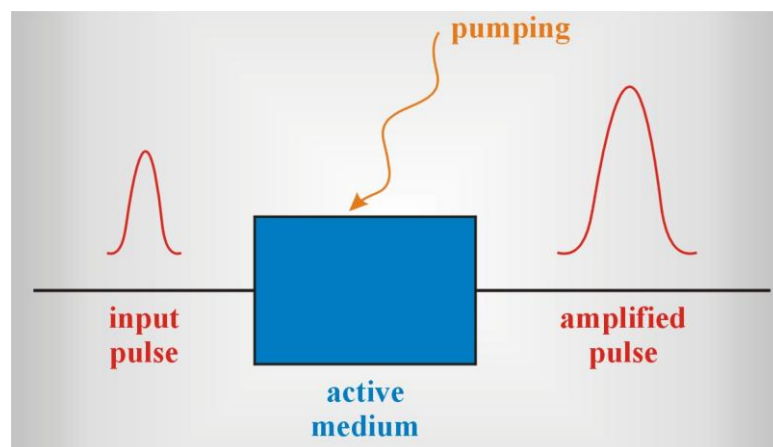


Fig. 7.28 Illustration of amplification

Let us consider a mechanism of amplification in the three-level system (Fig. 7.29)

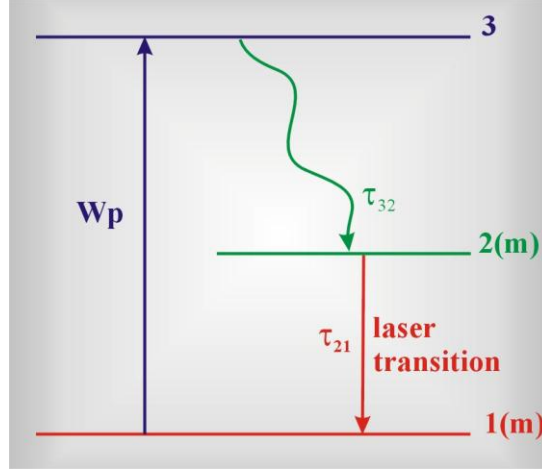


Fig. 7.29 Three-level system.

Let assume that the relaxation time  $\tau_{32}$  for the  $3 \rightarrow 2$  transition is short in comparison with the lifetime of the  $E_2$  state  $\tau_{21}$ , which is a good approximation in solid-state lasers. This denotes that the number of molecules  $N_3$  occupying the level  $E_3$  is negligible compared with the number of molecules in  $N_1$  and  $N_2$  ( $N_3 \approx 0$ , and  $N_1 + N_2 = N_0$ ) because the molecules are pumped almost immediately into the metastable level  $E_2$  with only a momentary stay in  $E_3$ . Basing on this assumption, the change in the population is

$$\frac{dN_2}{dt} = W(N_1 - N_2) - \frac{N_2}{\tau_{21}} + W_p N_1 \quad (7.42)$$

$$\frac{dN_1}{dt} = -\frac{dN_2}{dt} \quad (7.43)$$

where

$$W = B_{21}\rho. \quad (7.44)$$

Neglecting spontaneous emission and pumping  $W_p$  during the pulse duration, which is usually much shorter, the eq. (7.42) can be written in the form

$$\frac{dn}{dt} = -\gamma Wn, \quad (7.45)$$

where

$$n = N_1 - N_2 \quad (7.46)$$

denotes the population inversion,  $\gamma = 1 + \frac{g_2}{g_1}$  (for three-level system, where  $g_2, g_1$  are the degeneration numbers). One can show<sup>6.1</sup> that

$$W = \frac{\sigma I}{h\nu} \quad (7.47)$$

where  $\sigma$  [ $\text{cm}^2$ ] is the stimulated emission cross section,  $I$  is the radiation intensity  $\left[ \frac{\text{J}}{\text{s cm}^2} \right]$ ,  $\nu$  is the frequency of the  $2 \rightarrow 1$  transition. Substituting (7.47) into (7.45) and expressing the intensity in terms of the photon density  $\phi$  [ $\text{photons/cm}^3$ ]

$$\frac{I}{h\nu c} = \phi, \quad (7.48)$$

one gets

$$\frac{dn}{dt} = -\gamma c \sigma n \phi. \quad (7.49)$$

The rate at which the photon density changes in a small volume at  $x$  of an active medium is equal to

$$\frac{\partial \phi}{\partial t} = Wn - \frac{\partial \phi}{\partial x} c \quad (7.50)$$

where the first term describes the number of photons generated by the stimulated emission and the second term – the flux of photons which flows out from that region.

Using once again (7.47) and (7.48) in (7.50) one gets

$$\frac{\partial \phi}{\partial t} = cn \sigma \phi - \frac{\partial \phi}{\partial x} c. \quad (7.51)$$

Using the differential equations (7.49) and (7.51) one can solve them for various types of the input pulse shapes<sup>6.2, 6.3</sup>. For a square pulse of duration  $t_p$  and the initial photon density  $\phi_0$  one obtains:

$$\frac{\phi(x, t)}{\phi_0} = \left\{ 1 - [1 - \exp(-\sigma n x)] \exp \left[ -\gamma \sigma \phi_0 \left( c \left( t - \frac{x}{c} \right) \right) \right] \right\}^{-1}. \quad (7.52)$$

After passing through an active medium of length  $x = L$  the amplification is given by

$$G = \frac{\int_{-\infty}^{\infty} \phi(L, t) dt}{\phi_0 t_p}. \quad (7.53)$$

After substituting (7.52) into (7.53) and integrating one gets

$$G = \frac{1}{c \gamma \sigma \phi_0 t_p} \ln \left\{ 1 + [\exp(\gamma \sigma \phi_0 \tau_0 c) - 1] e^{n \sigma L} \right\}. \quad (7.54)$$

The equation (7.54) can be cast in a different form using the input energy  $E_{in}$

$$E_{in} = c \phi_0 t_p h \nu, \quad (7.55)$$

and the saturation fluence that we defined in chapter 1 (eq. 1.39)

$$E_s = \frac{h \nu}{\gamma \sigma} = \frac{E_{st}}{\gamma g_0}, \quad (7.56)$$

where  $E_{st} = h \nu n$  is the energy stored per volume,  $g_0 = n \sigma$  is the small signal gain coefficient (see chapter 1, eq. 1.23). Using the expressions for  $E_{in}$  and  $E_s$  in (7.54) one obtains the energy gain  $G$

$$G = \frac{E_s}{E_{in}} \ln \left\{ 1 + \left[ \exp \left( \frac{E_{in}}{E_s} \right) - 1 \right] G_0 \right\}, \quad (7.57)$$

where  $G_0 = \exp(g_0 L)$  is the small-signal single-pass gain.

Let us consider limit cases:

- The input signal is low,  $E_{in}/E_s \ll 1$ . The eq. (7.57) can be approximated to the exponential dependence on the active medium length  $L$

$$G \cong G_0 = \exp(g_0 L). \quad (7.58)$$



- The high input signal,  $E_{in}/E_s \gg 1$ . Then, eq. (7.57) becomes

$$G \cong 1 + \frac{E_s}{E_{in}} g_0 L \quad (7.59)$$

with the linear dependence of the energy gain.

## 7.2.2. Optical amplifiers

Optical amplifiers can be divided into the following groups

- rare earth elements doped fiber amplifiers (erbium - EDFA, 1500-1600 nm or praseodymium - PDFA, 1300 nm)
- semi-conductor optical amplifiers SOA, 400-2000 nm
- Raman amplifiers (description of Raman amplifiers)
- Brillouin amplifiers

### 7.2.2.1. Erbium doped fiber amplifier EDFA

Optical amplifier is the piece of fiber doped with a rare earth element, most often it is erbium, pumped by the laser diode through a coupler (fig.7.30) .

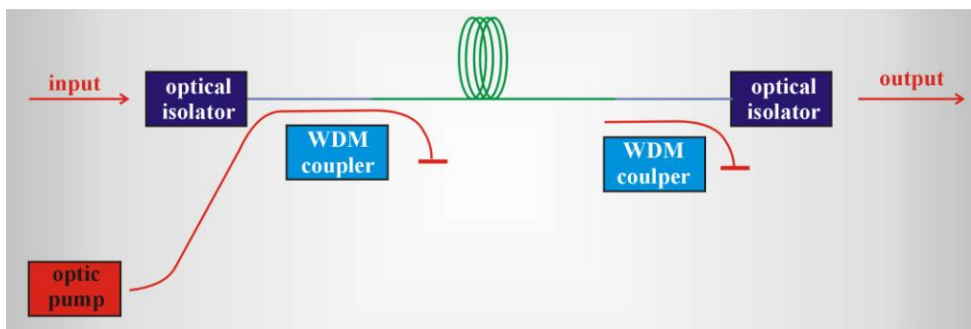


Fig. 7.30 Typical commercial EDFA amplifiers

Optical amplifying takes place on electron levels of rare earth elements (erbium, holmium, neodymium, samarium, thulium, ytterbium). The parameters of optical amplifiers, such as the wavelength or the gain band depend on properties of doped elements firstly, not on the glass of a fiber, which plays first of all the role of a matrix. The erbium doped amplifiers EDFA use three level scheme of pumping and electron energy dissipation (fig. 7.31). The amorphous nature of silica glass has an influence on gain spectrum because it causes broadening of the electron levels of erbium  $Er^{+3}$ .

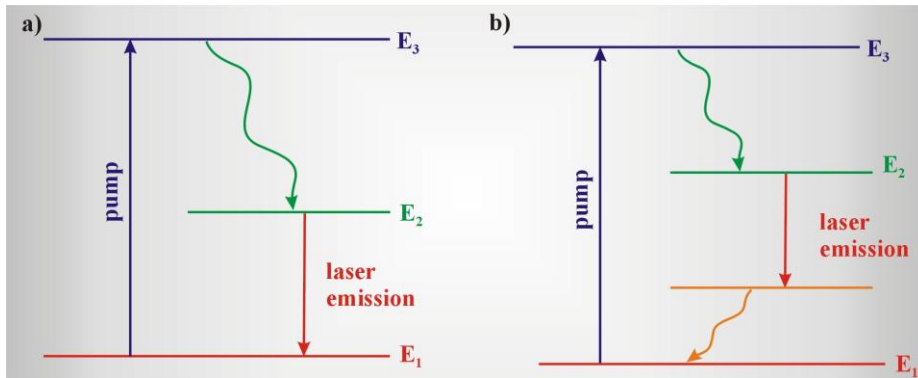


Fig. 7.31 Three level scheme of pumping and electron energy dissipation in erbium amplifier

To get the amplification, erbium ions must be pumped to the higher energy state and then they must dissipate their energy to a metastable state. The pumping of erbium of  $Er^{+3}$  is possible with different wavelengths as it is shown in Fig. 7.31. The most often used wavelengths of pumping are 1480 nm and 980 nm, allowing to reach amplification on the order of 30-40 dB for pumping power of about 10 mW. In the erbium amplifier we can apply configuration with forward pumping, in which the amplified and pumping beams have the same direction or they are opposite directed (backward pumping) as well as pumped from both sides (Fig. 7.32)

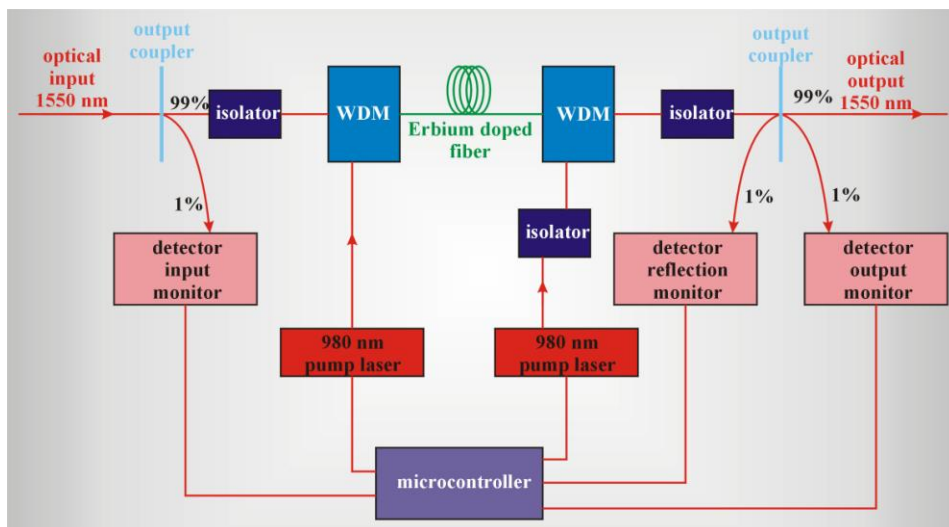


Fig. 7.32 Erbium doped fiber amplifier EDFA pumped from both sides.

For small pumping powers, when amplifier works below saturation level, both ways of pumping are equally effective. For large pumping powers, when amplifier works at the saturation regime - backward pumping is more effective because of lower amplified spontaneous emission ASE.

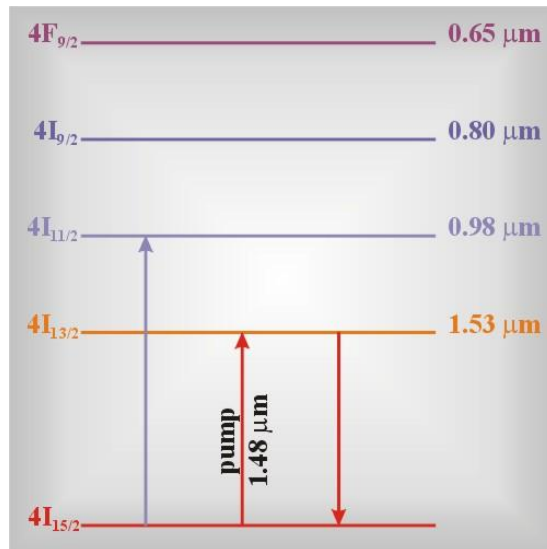


Fig. 7.33 Electronic states of erbium ion Er<sup>3+</sup>

Once upon the pumping the erbium ions become promoted to the excited state characterized by a short lifetime, and then as a result of radiationless transition they are transferred to a metastable state with long lifetime - about 10 ms. The excited ions return back to the ground level after about 10 ms emitting photons, in the process of the spontaneous and stimulated emission. As a result of stimulated emission photons at wavelength of 1550 nm are generated which have the same frequency, phase, polarization, direction, and the signal amplification takes place at 1550 nm (Figs. 7.33 and 7.34). The amplifying mechanism is the same as in lasers. In fact, optical amplifier can be regarded as a laser without optical feedback.

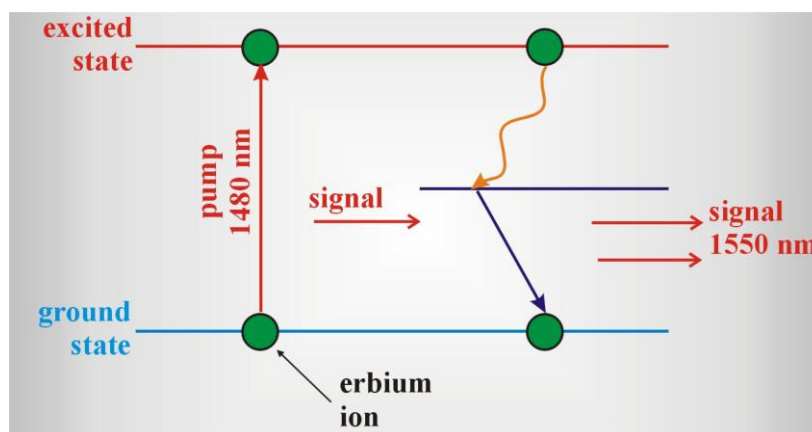


Fig. 7.34 Electron transitions in EDFA amplifier, three level system, pumping 1-2, radiationless transition 2-3, emission 3-1

The gain spectrum for an isolated doped atom (in this case erbium ion) for homogenously broadened band, caused by *dephasing processes*  $T_2$  (which were discussed in details in book [1]), is shown in the form

$$g(\omega) = \frac{g_0}{1 + (\omega - \omega_0)^2 T_2^2 + \frac{P}{P_s}} \quad (7.60)$$

where  $\omega_0$  is the value of gain in maximum,  $T_2$  is the dephasing time for doped element,  $P$  is the optical power of continuous signal CW (the continuous wave), which is strengthened,  $P_s$  is the saturation optical power. When amplifier works below level of saturations, that is when the condition is fulfilled

$$\frac{P}{P_s} \ll 1$$

formula (7.60) takes a form

$$g(\omega) = \frac{g_0}{1 + (\omega - \omega_0)^2 T_2^2} \quad (7.61)$$

This means that the amplifying is described by Lorentz function, for which the spectral width FWHM (full width at half maximum) is given by

$$\Delta\nu_g = \frac{\Delta\omega_g}{2\pi} = \frac{1}{\pi T_2} \quad (7.62)$$

Typical values of  $T_2$  are of about 0.1 ps, which gives typical broadening  $\Delta\nu_g$  of 3 THz that corresponds to 24 nm at maximum 1550 nm. The typical spectral widths of optical amplifier due to homogeneous broadening are of the order 4 -10 nm. In the multiplexing techniques WDM one optical amplifier gains many channels (wavelengths) simultaneously. Therefore, the wider the amplified band, the better operation. For EDFA amplifiers the amorphous nature of silica glass has influence on the gain spectrum because it causes additional inhomogeneous broadening of electron levels of erbium  $\text{Er}^{+3}$ . Fig. 7.34 presents the absorption spectrum and gain spectrum of erbium in the silica fiber.

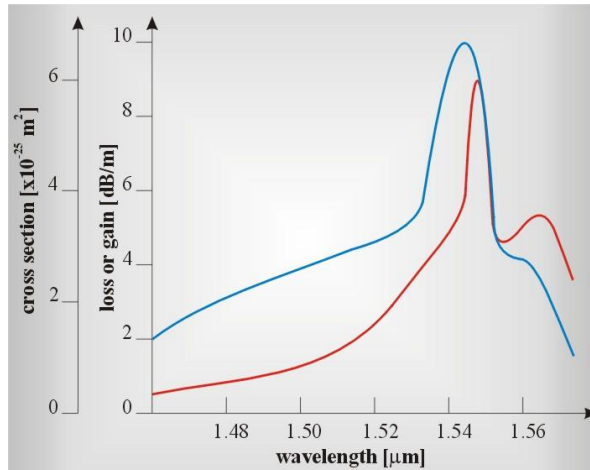


Fig. 7.35 Absorption and gain spectra of erbium in silica fiber [9].

As we can see from Fig. 7.35 inhomogeneous broadening causes that the gain spectrum is wide and has double structure. The later feature is not profitable as the ideal gain spectrum should be flat and wavelength independent. Otherwise, different WDM channels

will be gained differently and it will lead to considerable disturbance of system work. Therefore, the ideal amplifier for telecommunication aims is an amplifier with flat, broad and wavelength independent gain spectrum. It turns out, that the gain band of silica doped with aluminum Al, phosphorus P, germanium Ge, calcium Ca becomes considerably inhomogeneously broadened, even up to 80 nm, flattened at maximum with vanished double structure (Fig. 7.36).

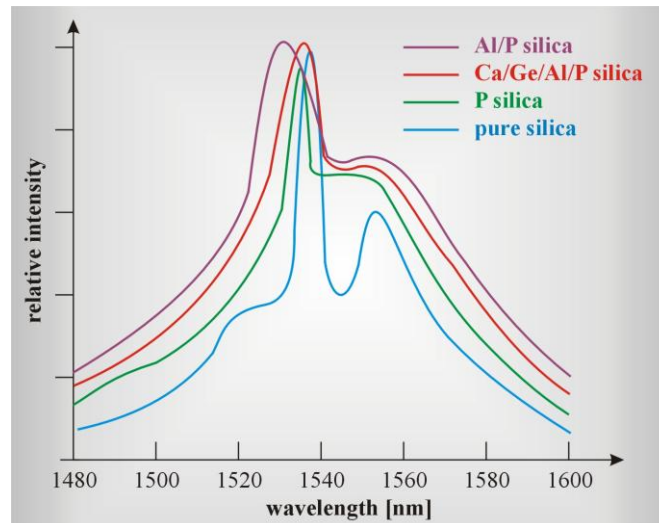


Fig. 7.36 The gain spectrum of EDFA amplifier doped with Al , Ca, P. Adopted from [9]

In practice, it is possible to reach the flat band profile of EDFA amplifier on the order of 30 nm by applying filters, Mach - Zehnder modulators and other optical devices. The width of 30 nm is sufficient for WDM systems with the number of channels smaller than 50. Recent DWDM and UWDM employ 160, and even 320 channels and the width 30nm is not sufficient. To increase the width of the gain band we often apply two-stage amplifying system which consists of two variously doped (first-erbium, second- additionally ytterbium and phosphorus doped) amplifiers set in row which can assure the gain from 1540 to 1560 nm. Another solutions combine EDFA amplifier with Raman amplifier, which will be discussed later. Such a combination gives over 65 nm gain width permitting to gain in the range from 1549 to 1614 nm [7]. Such amplifiers can work in large part of the band C (1530-1560 nm) and band L (1570-1600 nm) (Fig. 7.36a).

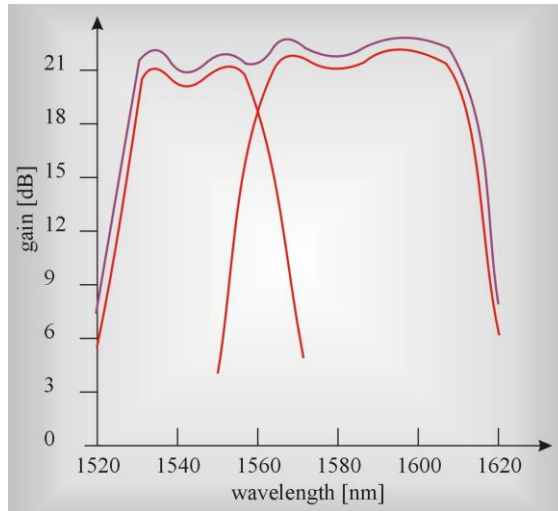
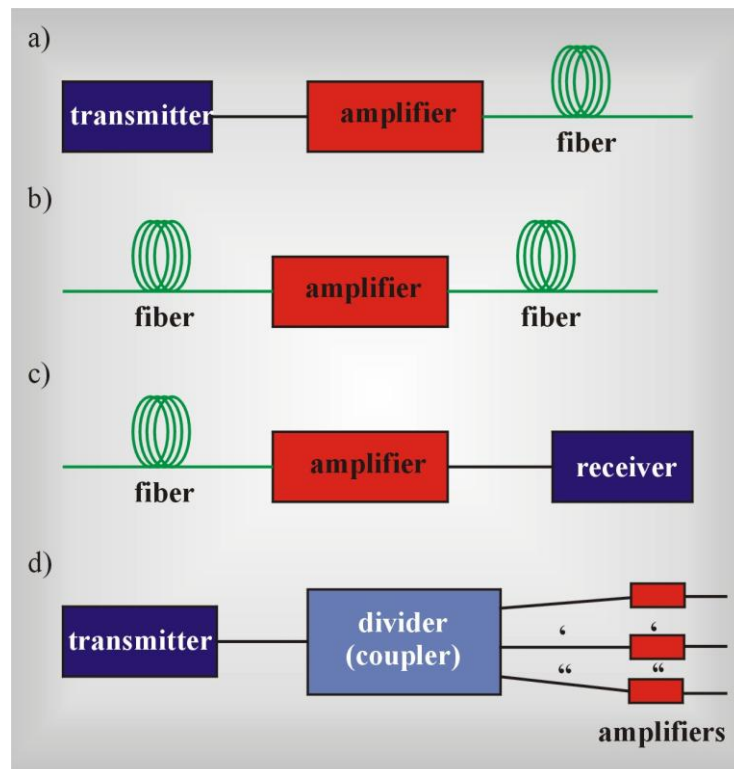


Fig. 7.36a The gain spectrum for the hybrid optical amplifier (EDFA+Raman). Line shifted up 1 dB to obtain larger transparency of drawing presents the total gain of the hybrid amplifier. Adopted from [9]

Optical erbium amplifiers EDFA are employed in different parts of the telecommunication net (Fig. 7.37). They are used as

- booster amplifier
- intermediate amplifier
- pre-amplifier
- cascaded amplifiers



- Fig. 7.37 Types of optical amplifiers , a) booster, b) intermediate amplifier, c) pre-amplifier, d) cascaded amplifiers
- 

*The booster amplifier* is placed directly after optical transmitter in order to receive a large input signal directed to the fiber. The *intermediate amplifier* regenerates the optical power that decreases due to attenuation in a fiber . The intermediate amplifiers are set in a row every tens kilometers. *The pre - amplifier* is placed before detector to gain the signal before detection. Recently applied high bit rates systems need the detector sensitivity on the level of -40 dBm, what requires the use of signal amplifiers before receiver. It introduces additional noises which are critical in this part of net because they have influence on the quality of transmission. The pre-amplifiers noises have to be small. *Cascaded amplifiers* are put in LAN nets just before the splitter (Fig. 7.38) to compensate the losses caused by the splitter.

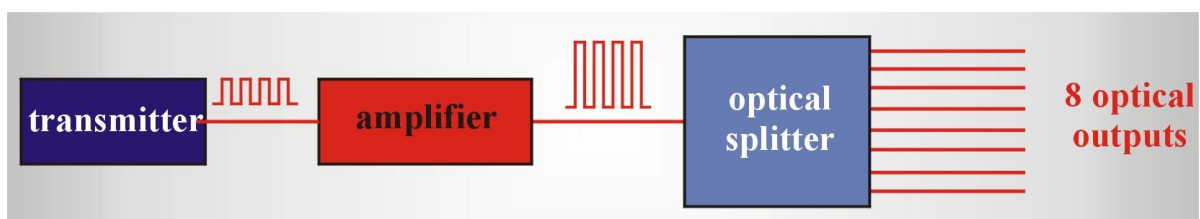


Fig. 7.38 Amplifiers compensating losses of a splitter.

For example, let us consider the splitter 1 x 8. Let the optical power of the transmitter to be 10 dBm, and typical losses caused by a splitter to be 10 dB. It means, that without the amplifier the signal entering the receiver would be 0dB (which corresponds to the power of 1 mW). Such a power would be sufficient for majority of digital applications, however in most of analog applications, eg. the CATV this power is on the bottom level of acceptability. If we put the amplifier before the splitter and a power after gain is 19 dB, each of 8 channels of a splitter receives 9dBm, which is almost equal to the power emitted from the transmitter.

### 7.2.2.2. Raman amplifier [10]

Although Raman gain is well-known since beginning of seventies [11] it was considered to be much less effective than the optical gain in EDFA amplifiers. Indeed, for small powers of the order 100 mW that were used in early WDM systems with 32 channels, the gain process of EDFA is considerably more effective than the Raman gain. However, when in 1999-2001 the number of channels grew up to 64-160, requirements to power increase also grew up. Higher powers, on the order of 200 mW were applied, for which the Raman gain begins to be competitive. Starting from 2002 when the number of channels grew up to 240 channels and more, powers significantly exceeded 200 mW, the Raman gain started to be much more effective than the EDFA gain (Fig. 7.39). Moreover, in EDFA amplifiers the saturation level is reached quickly, above which the output power does not grow up in spite of pumping power increase.



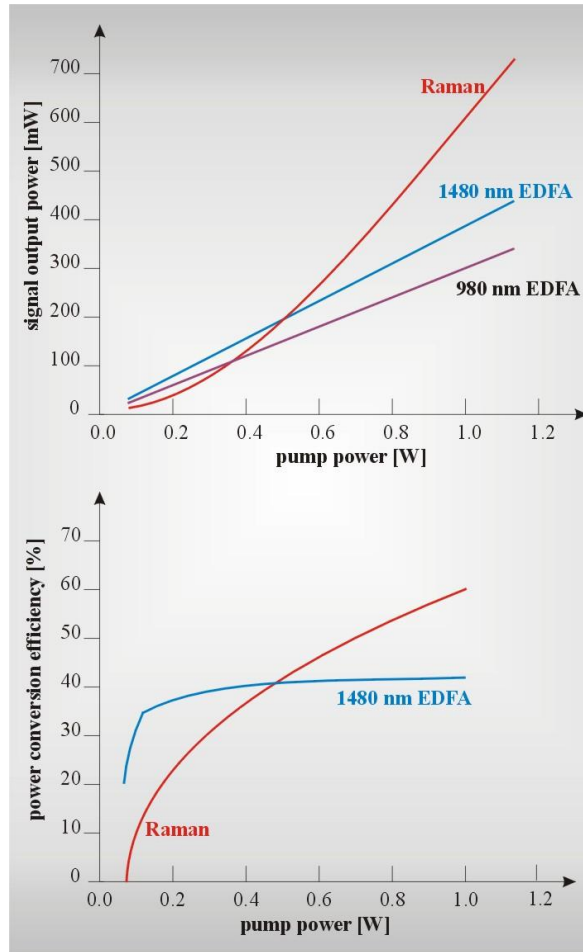


Fig. 7. 39 Input power versus pumping power in optical Ramana amplifier (a), power conversion efficiency PCE versus pumping power,  $PCE=(P_k-P_0)/P_0$  , where  $P_k$  is the output power,  $P_0$  is the input power. Adopted from [10]

EDFA amplifier acts like a laser on erbium electron transitions without optical feedback. Similarly, Raman amplifier can be treated as the Raman laser without optical feedback. The Raman lasers have been considered in chapter 5, while the Raman scattering phenomenon has been discussed in chapter 4.

Let us remain that the Stokes component, which is created as a result of Raman light scattering, and characterized by smaller energies than the incident photons because part of the photon energy is given to the vibrational degrees of freedom. The Stokes component has a frequency  $\omega_s = \omega_L - \omega_{wib}$ , shifted by the frequency of the vibration mode  $\omega_{wib}$  of material from which the fiber is built. For the glass fiber  $\omega_{wib}$  is about  $440\text{ cm}^{-1}$  (13.2 THz) and it corresponds to the vibrational mode of silica  $\text{SiO}_2$ . When the power of the pumping laser is sufficiently large and exceeds the threshold value the Raman scattering becomes the stimulated Raman scattering (SRS).

The advantages of Raman amplifiers can be summarized as follows:

- Raman gain takes place in every fiber, which permits to avoid the expensive material modifications,
- the gain is non-resonant, so it can be employed in the whole range of light penetrability in fibers, that is from 300 nm to 2000 nm,

- the gain band is comparatively wide and it is about 5 THz,
- Raman amplifiers have however some disadvantages with respect to EDFA amplifiers:
- lower efficiency for low powers ( $< 100$  mW), one requires longer fiber for gaining,
  - short response time (on the order of femtosecond).

Now we will show what the consequences of Stokes shift in a fiber in which light power is sufficient to trigger the effect of stimulated Raman scattering. Let us consider transmission in WDM systems with 6 channels in the III transmission window. Let the optical signals in individual channels have equal amplitudes as presented in Fig. 7.40.

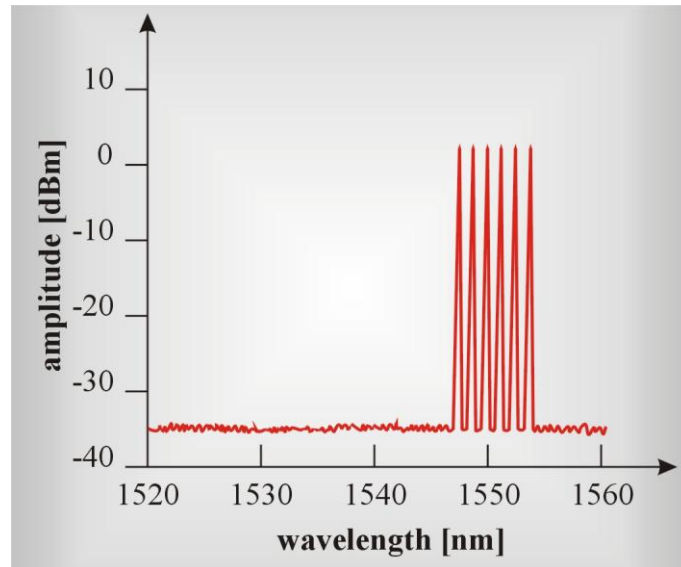


Fig. 7.40 Amplitudes and frequencies of WDM channels without stimulated Raman scattering SRS

When the SRS phenomenon takes place in a fiber, the spectrum from Fig.7.40 undergoes distortion. The optical signals of higher energy pass part of the energy to the vibrational modes and the more blue-shifted Stokes components undergo amplifying and the transmitted spectrum looks as follows (Fig. 7.41).

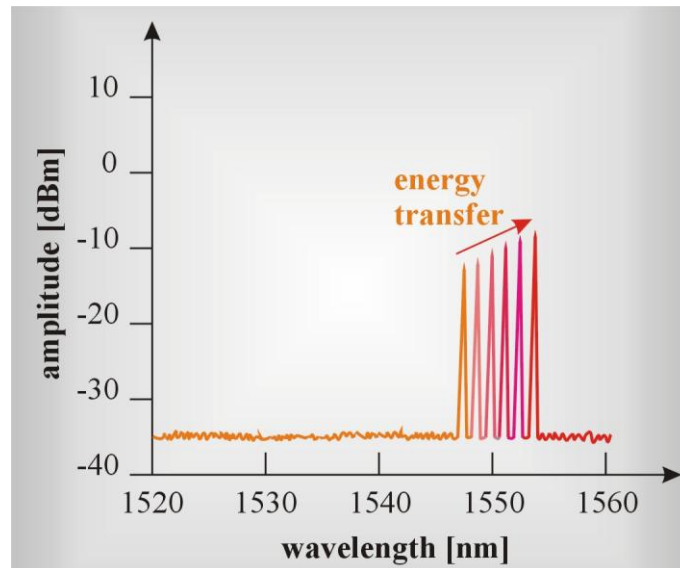


Fig. 7.41 Amplitudes and frequencies of WDM channels when stimulated Raman scattering SRS takes place in a fiber

When the fiber, in which stimulated Raman scattering SRS takes place, is pumped, eg. by the wavelength of 1535 nm, the signal amplitudes undergoes amplification (Fig. 7.42).

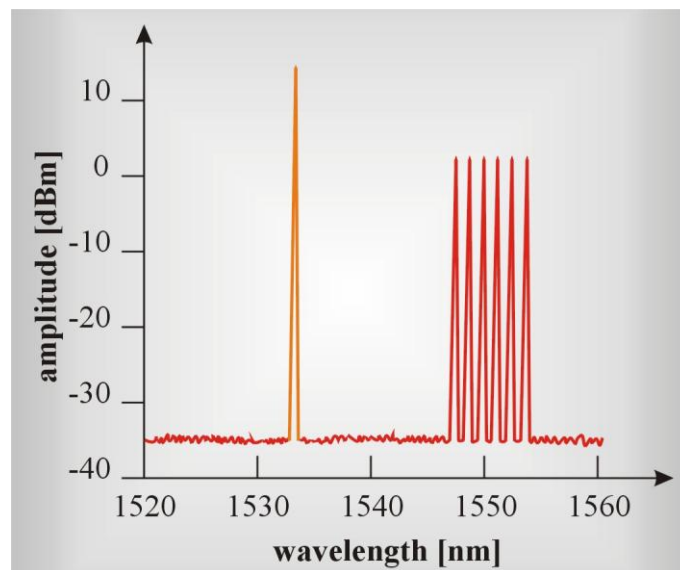
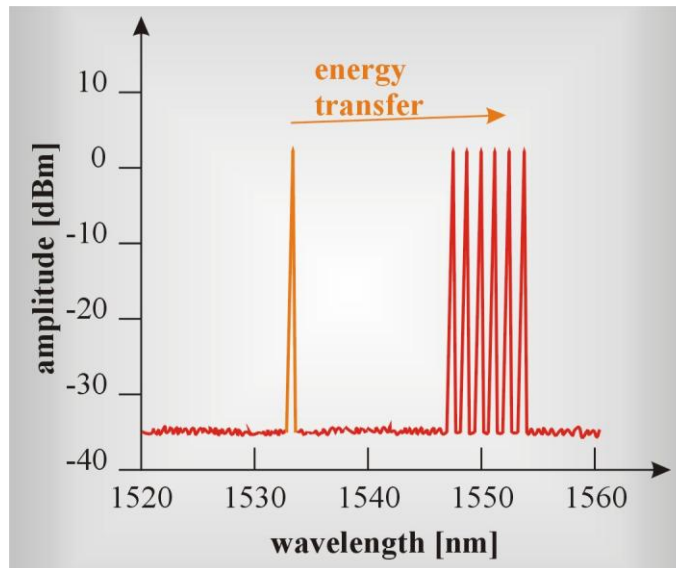


Fig. 7.42 Amplitudes and frequencies of WDM channels in Raman amplifier and a spectrum of the pumping signal 1535nm

When a signal propagates in a fiber, the pumping beam gives part of the energy to the WDM components of the signal and as a consequence the spectrum from the Raman amplifier looks like in Fig. 7.43.



**Fig. 7.43** Spectrum of amplitude and frequency of WDM channels in Raman amplifier and the spectrum of the pumping signal of 1535 nm received as a result of interaction the pumping beam with the transmitted signals.

Raman scattering is well-known for years. The breakthrough in the present gain application could have happened thanks to three factors:

- development of low dispersion fibers, in comparison with the standard single-mode fibers (SMF) the amplification grows up to 10 times,
- development of large power transmitters, present laser diodes deliver a power higher than 300 mW, optical lasers (cladding - pump fiber laser) deliver power > 10 W, the amplification grows up to 100 times,
- development of fiber components such as the diffractive grating, couplers, multiplexers etc.

Raman amplifiers can be divided into:

- co-propagating, signal and pumping beam is spread in the same direction, as a source of light Fabry – Perot diodes are usually used (they have lower relative intensity noise RIN than lasers with stabilized frequency)
- counter propagating, signal and pumping beam spread in opposite directions.

Another classification is related to

- distributed Raman amplifiers DRA, in which a pumping beam travels through transmission fiber (Fig. 7.44),
- discrete Raman amplifiers DRA or lumped Raman amplifiers LRA, which consist of a piece of fiber acting as an amplifier that is included into a transmission fiber (Fig. 7.45)

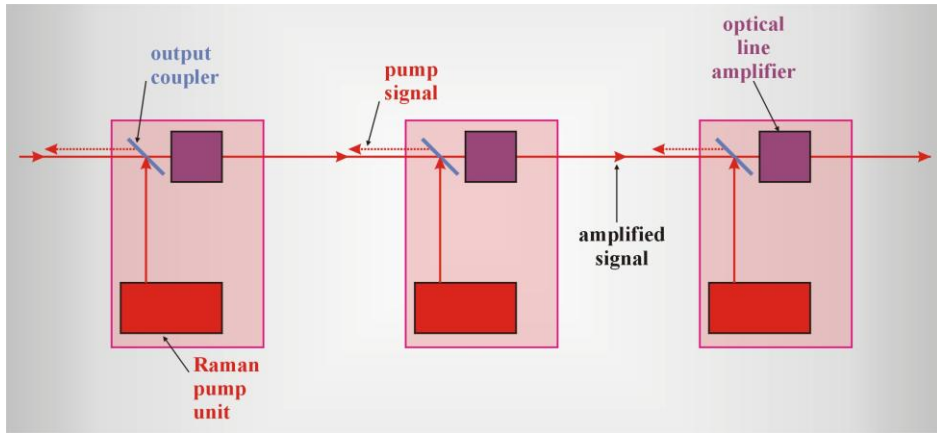


Fig. 7.44 Raman amplifier of DRA type

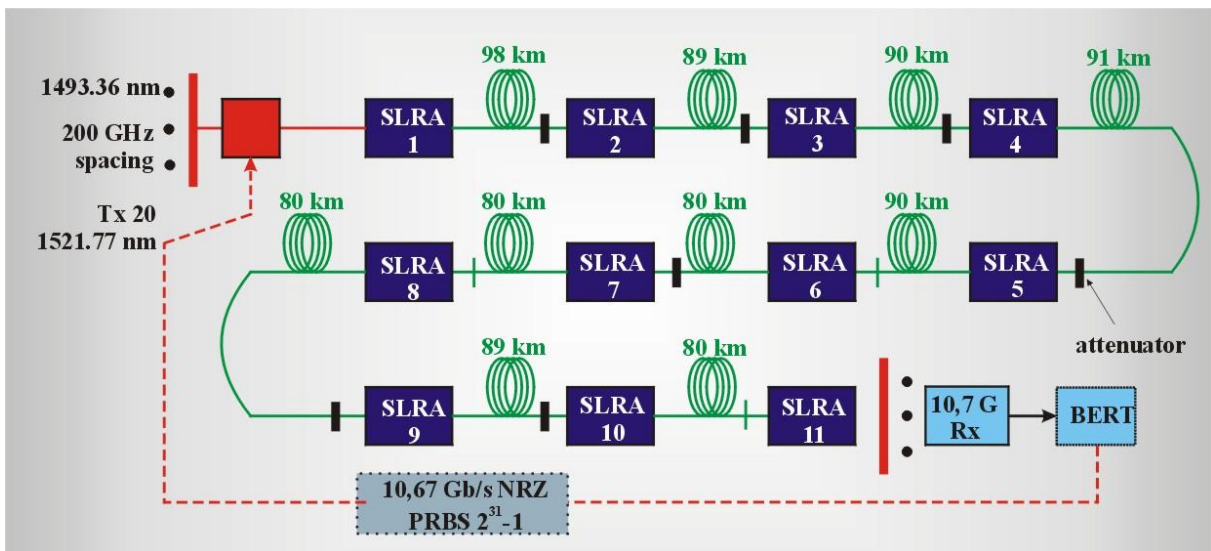


Fig. 7.45. Experimental system based on LRA amplifiers. Adopted from [10]

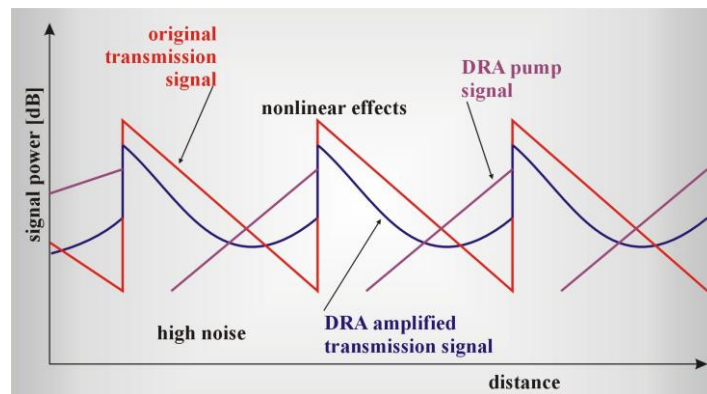


Fig. 7.46 Comparison of signal gained in DRA amplifier and in LRA amplifier .

In Fig.7.46 signals gained in Raman amplifiers of DRA and LRA types have been compared. The figure illustrates the superiority of DRA gain in comparison to periodical gaining at every tens kilometers which take place in amplifiers of LRA (as well as in EDFA).

Periodical gain has the shape of saw teeth with large amplifying at the beginning of a fiber after LRA amplifier and weak signal at the end. Signal from DRA is subjected to smaller fluctuations as gain appears on the whole length of the transmission fiber. The DRA amplifiers DRA are characterized with higher signal to noise ratio (SNR). Moreover, the maximum of gain signal at the pumping site do not have to be as high as for LRA, so the pump power can be lower, and as a result the non - linear effects are considerably reduced in DRA.

Fig. 7.47 presents the experimental system of gain of a signal modulated with velocity of 10.67 Gb/s by 11 amplifiers of LRA for 20 channels contained in range of 1493.36 nm - 1521.77 nm of the S band. The space between the channels is 200GHz and the total length of a fiber is 867 km. Losses were 21 dB, while the total output power was 14 dBm. Fig.7.47 presents the spectrum obtained after last stage of amplification, average SNR at width 01. nm was 20.7 dB, bit error rate BER < 10<sup>-12</sup> .

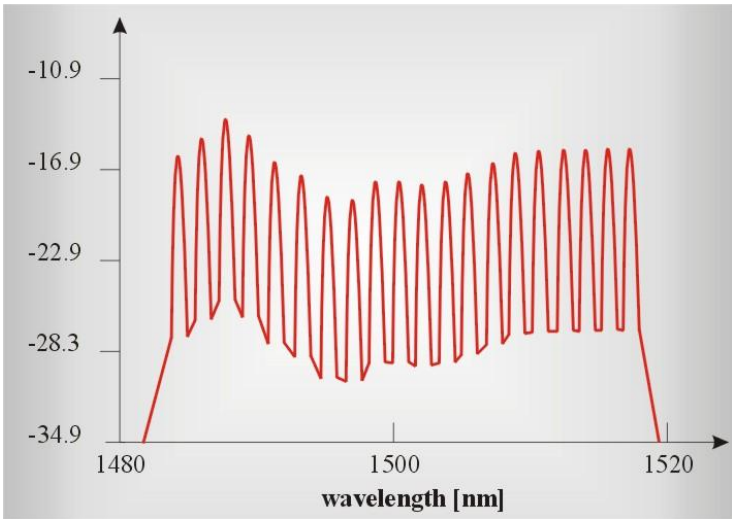


Fig. 7.47 Spectrum obtained after the last stage of amplification in experimental system from Fig. 7.45 , average SNR at width 0.1 nm was 20.7 dB, bit error rate BER < 10<sup>-12</sup> [10].

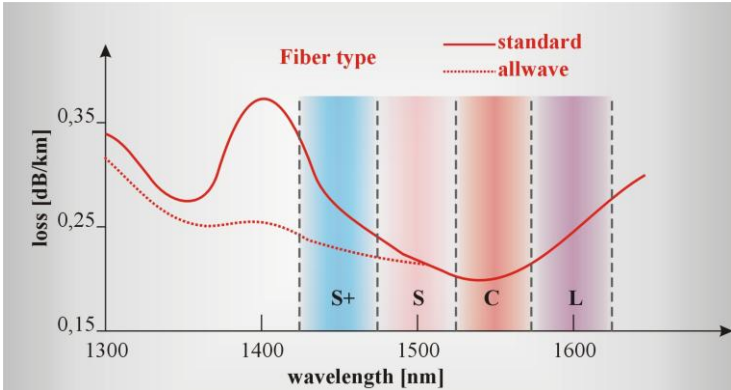


Fig. 7.48 Bands used in a fiber transmission

Raman amplifiers are used in optical platforms for signals propagating on huge distances. Recently applied Raman amplifiers are characterized by higher efficiencies than

EDFA amplifiers, even those the most effective, which are pumped with 1480 nm, not only 980 nm. Moreover, Raman amplifiers penetrate new spectral ranges, which are inaccessible for EDFA. EDFA gain in C band (1530 -1565 nm) and L ( 1565-1625 nm). Raman amplifiers can work in S band (1480 nm -1530 nm), S + (1430-1480 nm) and in the II transmission window (1280-1340 nm). Moreover, Raman amplifiers can work in the range of water peak (1390 nm) in fibers, in which the attenuation connected with water absorption was reduced by special drying technologies. Therefore, Raman amplifiers can work in the range from 1280 to 1530 nm, which is inaccessible for EDFA amplifiers.

Fibers can gain a weak signal if the strong pumping light would be introduced simultaneously, and their frequency difference lies in the range of Raman gain spectrum. The gain maximum is obtained, when this difference is equal to the maximum of the Raman gain spectrum. The Raman gain spectrum corresponds to the Raman spectrum of the vibrational band of the material from which the fiber is made. For the glass fiber this difference is about  $433 \text{ cm}^{-1}$  (13.2 THz) and it corresponds to the vibrational mode of silica  $\text{SiO}_2$ . The band of the vibrational mode is wide (about 5 THz) as a glass is amorphous, non - crystalline material and the spectrum corresponds to inhomogenous broadening of the Raman band. The gain takes place after reaching a threshold value, similarly as for laser action.

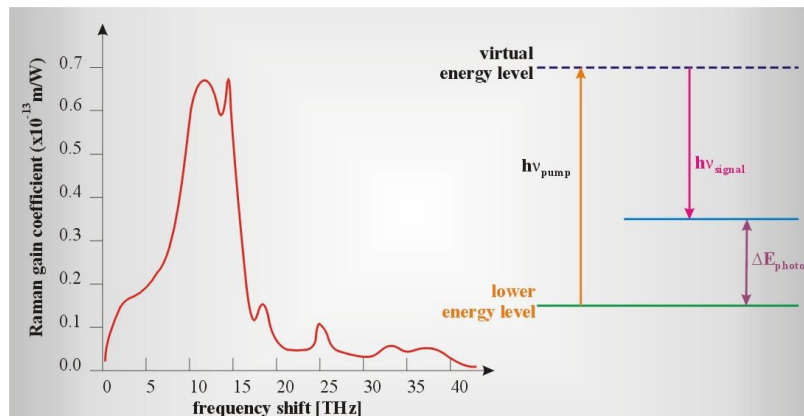


Fig. 7.49 Raman spectrum for fused silica  $\text{SiO}_2$ . The profile of Raman gain coefficient, wavelength of pumping beam  $\lambda_p=1550 \text{ nm}$  [10]

### 7.2.3. Semi-conductor amplifier

Semi-conductor optical amplifier looks like the diode laser, we have considered in chapter 5. The principles of operation of the semi-conductor amplifier are identical to the diode laser, with only difference, that there is no optical feedback (Fig. 7.50).

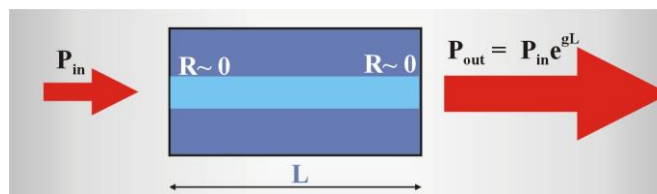


Fig. 7.50 Scheme of SOA (semiconductor optical amplifier)

Semi-conductor amplifier has a very small size and is coupled from both sides with the fibers (Fig. 7.51). The miniature sizes are their advantage, their disadvantage in



comparison with EDFA amplifiers are large power losses during coupling, polarization dependence and comparatively large noises.

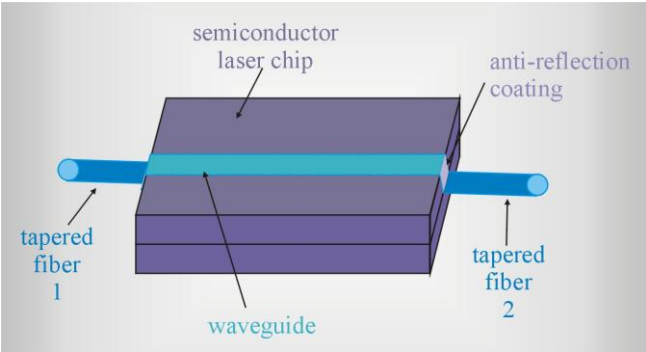


Fig. 7.51 Semi-conductor optical amplifier

Fig. 7.52 presents the application of semi-conductor technology in switches (a), wavelength converters (b), and (de)multiplexers.

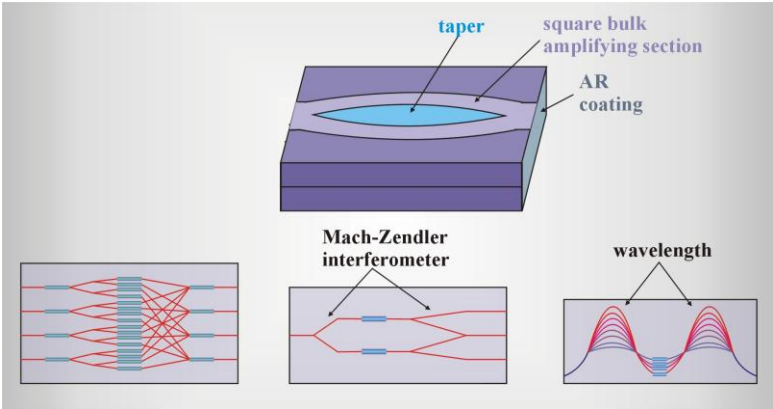


Fig.7.52 Applications of semi-conductor technology in switches (a), wavelength converters (b), and (de)multiplexers by integrating of semi-conductor optic amplifier with coupler or with the Mach -Zehnder interferometer. Adopted from Alcatel, Optical Networks Tutorial



## 7.2.4. Modulators

We will deal with group of devices which modulate light transmitted in a fiber. The light modulation plays a key role in optical transmission. The continuous light that has the same intensity with time does not bring any information. The direct modulation of a light that is emitted from the LED diode or diode laser takes place by modulation of electric current forward applied to the light source. Fig. 7.52. presents the basic methods of modulation - rectangular signal (on-off modulation) or intensity changing linearly between two defined levels.

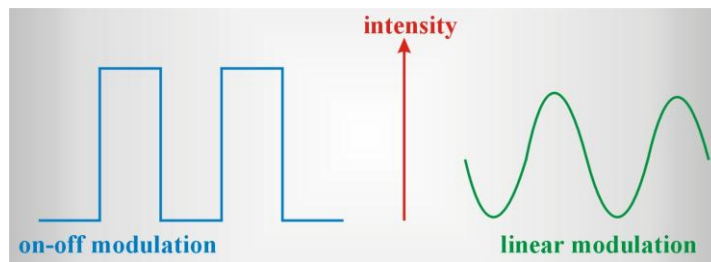


Fig. 7.53 Basic ways of light modulation

The simplest ways of modulation is shown in Fig. 7.53. Digital modulation of on/off type can get different forms, the simplest way is the modulation in which the pulse denotes the logical value of "1", while the lack of the pulse denotes "0".

In contrast, the linear modulation is used in analog transmission. The analog modulator is characterized by the following parameters:

- $P_{MAX}$ ,  $P_{MIN}$  - maximum and minimum value of modulated light power, the minimum value is usually 5% of the maximum value,
- $V_p$  – voltage applied to one branch, to get phase shifting by  $180^\circ$ ,
- Value of constant current around which oscillates the modulating signal,
- Losses, usually 3-5 dB, caused by modulation, to which we should add losses of the modulator, usually also 3 dB. The total losses are around 6-9dB.

The main disadvantage of the direct modulation is the chirp phenomenon, discussed in chapter 5, which is generated at the moment of the current switching on or off. The chirp is unfavorable, particularly for the large bit rate systems and in the WDM systems because it causes broadening of the spectrum emitted from the transmitter. This is the main reason why the direct modulation is replaced by the external devices, called modulators. In practice, when distances are larger than 100 km, and bit rates on the order of tens Gb/s, the direct modulation should be replaced by external modulation.

There is a wide range of modulators employing the following properties

- Opto-acoustic ( 100 MHz)
- Magneto-optic (200MHz)
- Electro-optic (GHz)
- Electro-absorption (GHz)

Each of the four types of modulators uses different way of interaction of light either with acoustic wave (optoacoustic modulators), with material whose properties are changed under the influence of electric field (electro-optic modulators and electroabsorption

modulators) or magnetic field (magnetic modulators). The numbers in brackets show the upper limit of modulation frequency.

Applications of these phenomena in optoelectronics are very wide, some of them have already been described in this book. In chapter 5 we described the optoacoustic phenomenon employed to generate the mode locking regime with a train of ultra-short pulses. The optoacoustic modulator is also used in pulsed lasers working in the Q-switching regime. The optoacoustic modulator is shown in Fig. 7.54. The optoacoustic modulators are usually made of tellurium dioxide  $\text{TeO}_2$  or lead molybdate  $\text{PbMoO}_4$ . The piezoelectric converters generating the optoacoustic wave in a modulator are made of lithium niobate  $\text{LiNbO}_3$ . They are characterized by a small steering voltage ( $\pm 15\text{V}$ ). The optoacoustic modulators are slower than the electrooptic modulators.

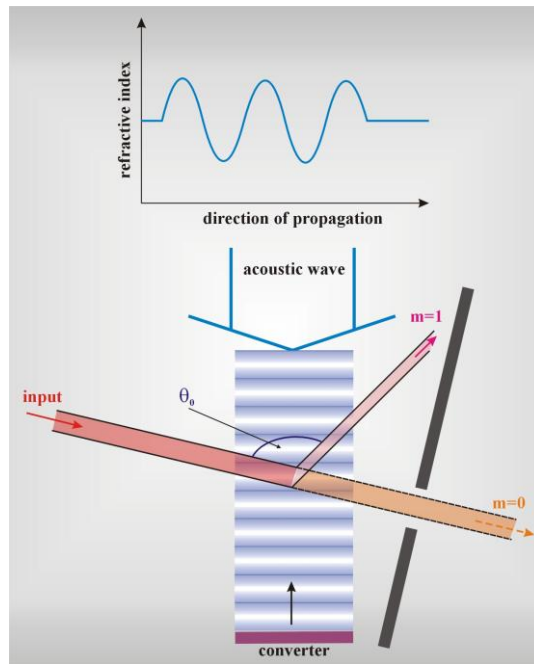


Fig. 7.54. Optoacoustic modulator

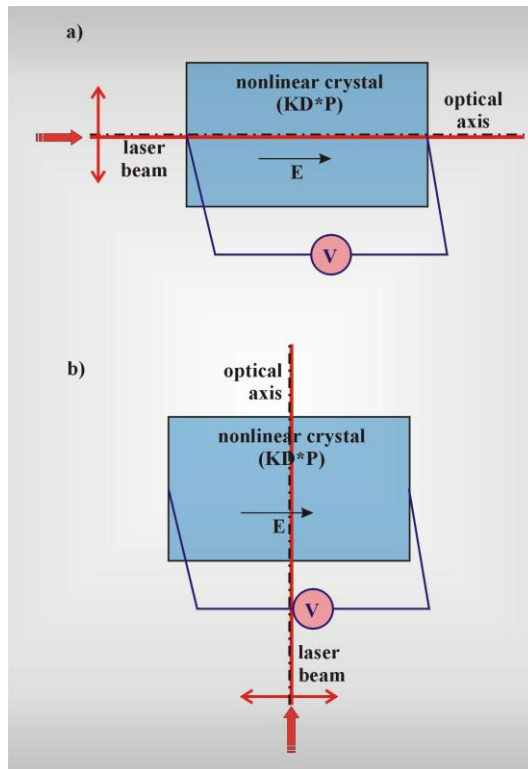
The magneto-optic modulator that employs the Faraday effect, and which finds its application in optical isolator, has been discussed in chapter 7.1.4.

Most of electro-optic modulators are based on two effects – **Pockels effect** and **Kerr effect**. The electrooptic effects in materials occur when the external electric field is applied. The external electric field generates the optical birefringence. It means that the electric field changes not only the value of the refraction index but also causes the change of material symmetry. Isotropic materials become anisotropic, single axis crystals become double axis crystals, e.g. When the change of the refraction index is a linear function of the external electric field - the electrooptic effect is called the Pockels effect. When the change is a nonlinear, second order dependence on the external electric field, it is the Kerr effect.

$$\Delta\left(\frac{1}{n^2}\right)_i = \sum_j^3 r_{ij} E_j + \sum_{jk}^3 R_{ijk} E_j E_k \quad (7.63)$$

### 7.2.4.1. Pockels and Kerr effects [5]

The Pockels cell plays an important role as an electro-optical  $Q$ -switch. Now we will explain its operation. The Pockels cell consists of a nonlinear optical material with the voltage applied to the material. The electric field can be applied along the direction of the laser beam (Fig. 7.55a) or perpendicularly to it (Fig. 7.55b).



**Fig. 7.55** The Pockels cell, the electric field can be applied along the direction of the optical beam (a) or perpendicularly to it (b)

The crystal becomes birefringent under the influence of the applied electric field. The crystal used for the parallel configuration (fig. 7.55a) is uniaxial in the absence of an electric field with the optical axis along  $z$  direction. The refraction index projects as a circle on a plane perpendicular to the optical axis (Fig. 7.56a).

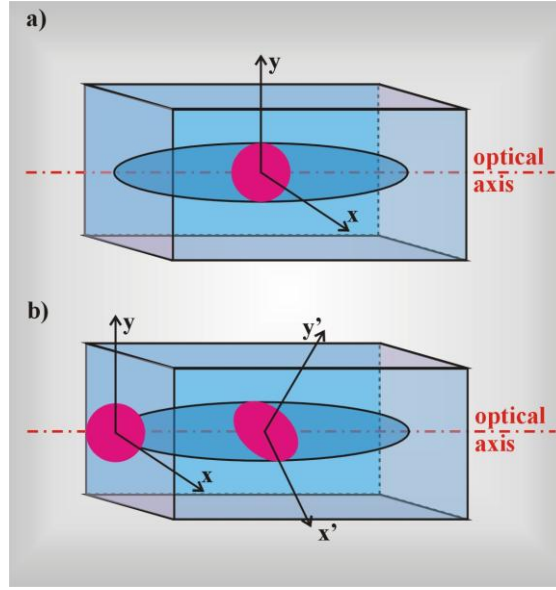


Fig. 7.56 Change of the refractive index in a  $\text{KD}^*\text{P}$  crystal,  $x, y, z$  – the crystallographic axes a) without an electric field, b) when an electric field is applied ( $E \neq 0$ ),  $x', y', z$  – the electrically induced axes

So, the laser beams having polarizations along  $x$  or  $y$  directions propagate with the same velocities along the  $z$  axis because the crystal is not birefringent in the direction of the optical axis. For the situation presented in Fig. 7.56a, the laser beam linearly polarized along  $y$  passes through the  $\text{KD}^*\text{P}$  crystal unchanged when no voltage is applied. When an electric field is applied along the crystal optical axis  $z$ , the refraction index projects as an ellipse, not a circle, on the plane perpendicular to the optical axis with the axes  $x'$  and  $y'$  rotating by  $45^\circ$  with respect to the  $x$  and  $y$  crystallographic axes (Fig. 7.56b). The angle of  $45^\circ$  is independent of the magnitude of the applied electric field. Therefore, when a voltage is applied, the  $\text{KD}^*\text{P}$  crystal becomes birefringent along the  $z$  axis, and divides the laser beam into two components (along  $x'$  and  $y'$ ) that travel through the crystal at different velocities. The polarization of the output beam depends on the phase difference between the two orthogonally polarized components – ordinary and extraordinary rays, which in turn depends on the applied voltage

$$\delta = \frac{2\pi}{\lambda} l \Delta n, \quad (7.64)$$

where  $\Delta n$  is the difference in the indices of refraction for the ordinary and extraordinary beams,  $l$  is the crystal length. It has been shown [6] that  $\Delta n$  can be expressed as

$$\Delta n = n_0^3 r_{63} E_z, \quad (7.65)$$

where  $r_{63}$  is the element of the electro-optic tensor of the third rank that is the response to the applied field  $E$  in the  $z$  direction ( $E_z$ ),  $n_0$  is the index of refraction for the ordinary ray. Employing the relation between the voltage  $V$  and the applied electric field  $E_z$ ,  $V_z = E_z l$  and inserting (7.65) in eq. (7.64) one gets

$$\delta = \frac{2\pi}{\lambda} n_0^3 r_{63} V_z. \quad (7.66)$$

When the applied voltage  $V_z$  is adjusted to generate the phase difference  $\delta = \pi/4$  or  $\delta = \pi/2$  the Pockels cell operates as a quarter-wave or half-wave plate.

The Pockels cell belongs to the fastest all-optical switching devices, and is highly reliable. Typical commercially available Pockels cells employ  $\text{KD}^*\text{P}$  crystals with  $\lambda/4$  voltage

between 3.5 and 4 kV at 0.69  $\mu\text{m}$  and 5 to 6 kV at 1.06  $\mu\text{m}$ . As a particular example, Pockels cells are used to select and retain high-peak-power pulses in regenerative amplifiers.

The Pockels modulator consists of an electrooptical crystal to which the modulating voltage is applied. It is placed between two polarization elements – polarizer and analyzer (Fig. 7.57).

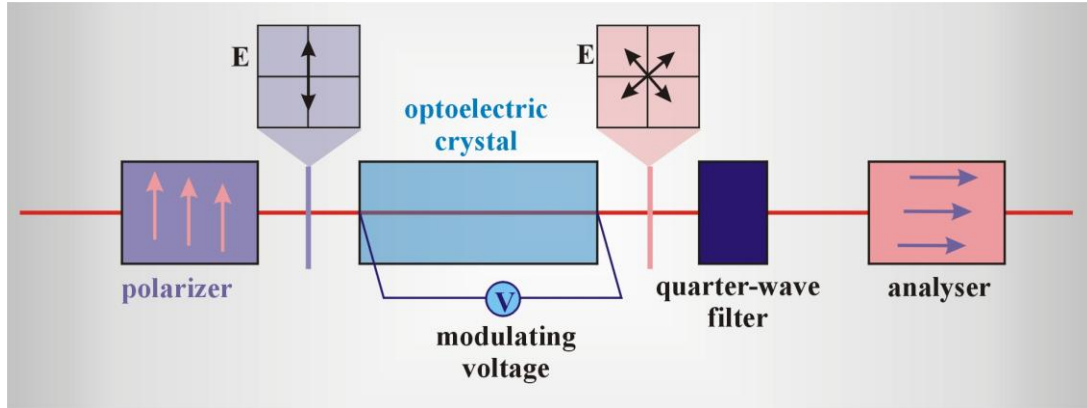


Fig.. 7.57 Pockels modulator

The Pockels modulator is the non-linear modulator, as the output signal  $I$  to input signal  $I_0$  ratio is expressed by formula [13]

$$\frac{I}{I_0} = \frac{\pi^2}{8} \left( \frac{V_0}{V_\pi} \right)^2 (1 + \cos 2\Omega t) \quad (7.67)$$

where  $\Omega$ ,  $V_0$ ,  $V_\pi$  are the modulation frequencies, amplitude of modulation voltage and half-wave voltage, respectively. The steering voltage  $V(t)$

$$V(t) = V_0 \cos \Omega t$$

is much smaller than the half-wave voltage. To make the Pockels modulator linear we can place quarter-wave plate between the polarizer and the Pockels cell. It introduces the additional shift of phase by  $\frac{\pi}{2}$  between the polarization components and the expression (7.67) gets the form

$$\frac{I}{I_0} = \frac{1}{2} [1 + \sin(\pi \frac{V}{V_\pi})] \quad (7.69)$$

so for small steering voltages the dependence becomes linear ( $\sin \alpha \approx \alpha$ ).

Fig. 7.58 presents the idea of Kerr effect applied to light intensity modulation.

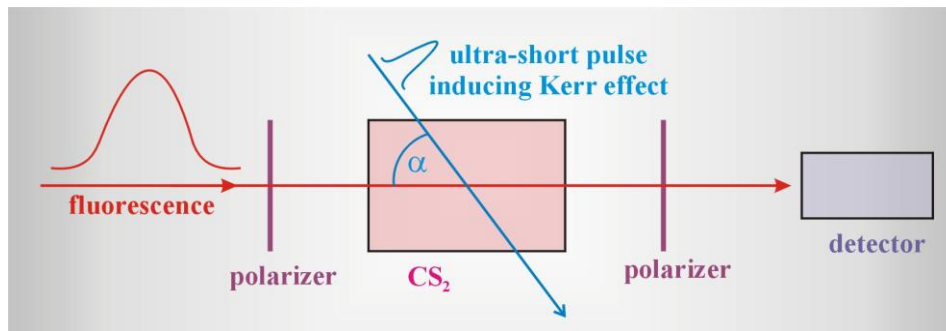


Fig. 7.58 Scheme illustrating the method of optical gating with use of Kerr effect

Let a material showing the third order electrooptic effect ( $R_{ijk} \neq 0$  in eq. (7.63)) (for example the carbon bisulphide ( $CS_2$ )) be placed between two crossed polarizers. In this case the light (for example, emitted as a result of fluorescence) will not reach the detector because the crossed polarizers block it. Carbon disulphide as an isotropic liquid and has no influence on polarization of the light. However, if we place the carbon bisulphide in strong electric field, molecules begin to align in direction of electric field and this arrangement causes that liquid become anisotropic with the distinguished optical axis and it begin to exhibit birefringence. The phenomenon birefringence generation in isotropic substances under the influence of electric field is known in literature as Kerr effect. In isotropic materials there is no Pockels effect, because the coefficient  $r_{ij} = 0$  (in eq. 7.63) for materials having the inversion centre. As a result of birefringence in liquid under the influence of electric field, the beam of light splits into two rays: ordinary and extraordinary, at polarization perpendicular to each other and the intensity dependent on the angle between the ray polarization and the direction of the optical axis. Moreover, the Kerr effect introduces the phase difference between the ordinary and extraordinary rays. As a consequence it alters the polarization of beam passing through the medium. If, instead of a constant electric field we apply an ultra-short laser pulse (Fig. 7.58), its electric field will induce short temporary Kerr effect. Liquid placed between the crossed polarizers, which before pulse appearing acts as the blocking screen, starts to act as the ultra fast shutter, which transmits fluorescent light for so long as liquid keeps birefringence induced by the pulse. It's time of about 3.5 picoseconds, so it is time of pulse duration and some additional time needed to change isotropic reorientation of molecules.

Modulators can also be divided according to the parameters they modulate:

- amplitude
- phase
- frequency

In conventional telecommunication systems the amplitude modulation is used, in coherent systems the modulation of phase and frequency is applied.

### 7.2.4.2. Mach – Zehnder modulator

Let us discuss another type of modulator that is based on electrooptical changes. Figure 7.59 illustrates the phase modulator, known as Mach-Zehnder interferometric modulator. Mach – Zehnder modulator uses the fact, that in electrooptical material the change of refraction index  $\Delta n$  caused by the external electric field of intensity  $E$  takes place and it is expressed by formula

$$\Delta n = 0.5n_0^3 r_{63} E \quad (7.69)$$

where  $n_0$  is the value of refraction index when  $E = 0$ ,  $r_{63}$  is the electrooptic coefficient. The change of the refraction index causes the change of phase of electromagnetic waves spreading in a fiber

$$\Delta\Phi = \frac{2\pi\nu\Delta n}{c} l = \frac{2\pi\Delta n}{\lambda} l \quad (7.70)$$

where  $l$  is the length of the optical path. Substituting (7.69) into (7.70) we get

$$\Delta\Phi = \frac{\pi n_0^3 r_{63} E}{\lambda_0} l = \frac{\pi n_0^3 r_{63} V}{\lambda_0 d} l \quad (7.71)$$

where the relation  $E = \frac{V}{d}$  has been applied,  $V$  is an applied voltage,  $d$  is a distance between electrodes. The Mach – Zehnder modulator consists of the splitter 1 x 2 and the coupler 2 x 1 creating the construction in shape of two letters Y. When the electric field intensity is off, the input light divides into two equal branches and it again joins in a coupler in the same phase. The output light has almost the same power. When the electric field is applied to one of the branches, the situation changes diametrically, because the refraction index has been changed. The input light separates into two beams and each of them propagates differently. The phase difference  $\Delta\Phi$  is generated as a result of different refraction indices in both branches of the fiber. When the voltage  $V$  is chosen in such a way that it generates the phase difference of  $180^\circ$  destructive interference takes place with the zero output intensity. The voltage on and off causes modulation of the light. The voltage  $V$ , which has to be applied to cause phase shift by  $180^\circ$  as a result of optical path difference  $\lambda/2$  can be derived from eq. (7.71) and is given by formula

$$V = \frac{\lambda d}{r_{63} n^3 L}$$

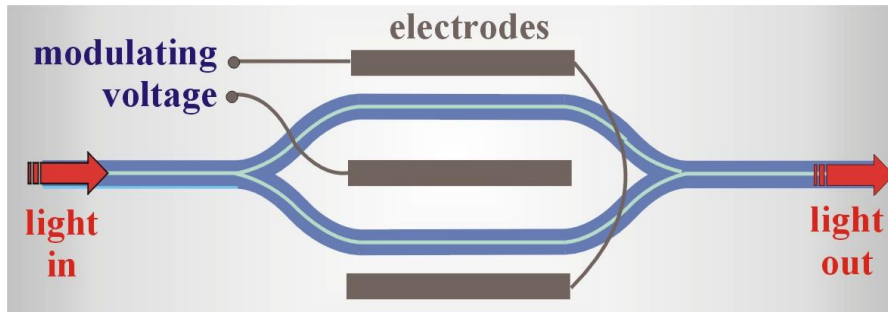


Fig. 7.59 Interferometric modulator of Y type (Mach-Zehnder)



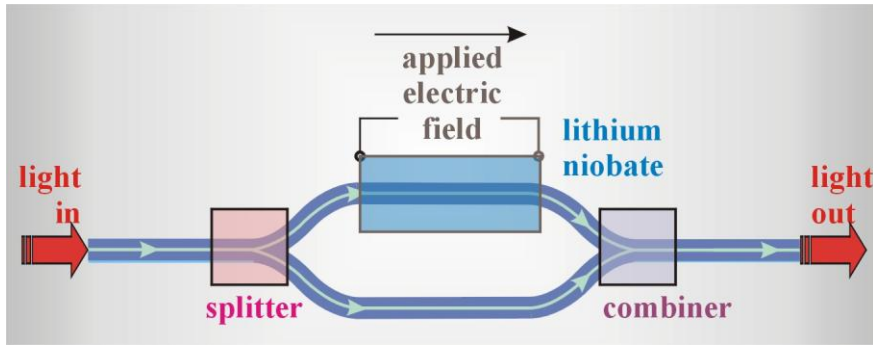


Fig. 7.60 Modulator of Y type with a crystal characterized by the large electrooptical coefficient

To enhance the phase modulation effect we can apply materials characterized by the large electrooptical coefficient (e.g.  $\text{LiNbO}_3$ ) or semi-conductor waveguides. The applied electric field alters a refraction index, the refraction index alters the velocity of light in the branch in which the crystal is placed and causes phase difference between the two branches. As a result, this phase difference causes modulation of light intensity. When phase difference is zero - light from both branches is added constructively and it has large intensity. When phase difference is  $180^\circ$  the light from both branches is added destructively and it has zero intensity. Mach-Zehnder modulators are applied as fast modulators in transmission systems with large bit rates on the order of Gb/s.

### 7.2.4.3. Semi-conductor modulator

The another type of modulator is presented in Fig. 7.61. This modulator employs electro-absorption phenomenon occurring in semi-conductor materials. We know that photons with energy larger than the value of the forbidden gap are absorbed and electrons are promoted from the valence band to the conduction band. The value of the energy gap can be modified by the applied electric field. To be more precise - the value of the absorption coefficient of the semi-conductor material is modified. The electric field  $E$  applied to the active semi-conductor layer causes shift of the absorption band to longer wavelengths according to formula

$$\alpha(h\nu, E) \propto \exp\left[-\frac{(E_g - h\nu)^{3/2}}{3eE}\right] \quad (7.72)$$

This effect is called **Franz – Keldysh effect** [14]. Semi-conductors quantum wells are particularly sensitive to electric field changes (Stark effect). Semi-conductors quantum wells are very thin semi-conductor layers on the order of few millimicrons. Light propagates through the optical fiber and then through area of the semi-conductor active layer. When the energy of propagating photons is lower than the forbidden gap – light propagating through semi-conductor isn't absorbed and it goes to the next fiber almost without losses. When we apply the backward biased electric field to the n-p junction, the value of the absorption coefficient increases – light is absorbed and its output intensity decreases (usually on the order of few percents). As a result, modulation of a voltage applied to semi-conductor causes change of absorption and modulation of light intensity. For typical semi-conductor materials



AlGaAs, GaAs, InP a typical electric field which should be applied to cause the absorption band shift is 100-600 kV/cm. It indicates that the Franz-Keldysh effect usually requires hundreds of volts, limiting its usefulness with conventional electronics.

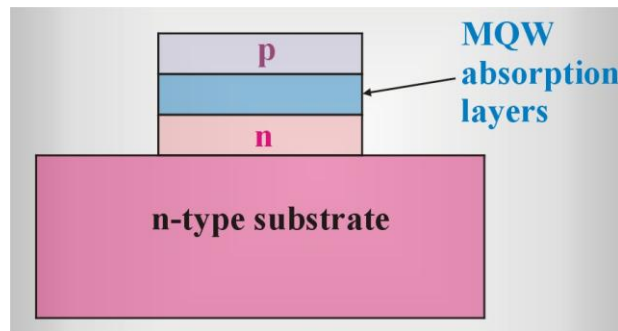


Fig. 7.61 Semi-conductor electroabsorption modulator

### 7.2.5. Multiplexers i demultiplexers

Optical multiplexer or demultiplexer are devices used in wavelength-division multiplexing systems for multiplexing and routing different channels of light into or out of a single mode fiber. The multiplexer links signals of various wavelengths transmitted through separate optical fibers into one fiber in which all signals propagate (Fig. 7.62). The demultiplexer performs the opposite operation - it separates signals corresponding to a single channel a single wavelength) from a stream of various wavelengths.

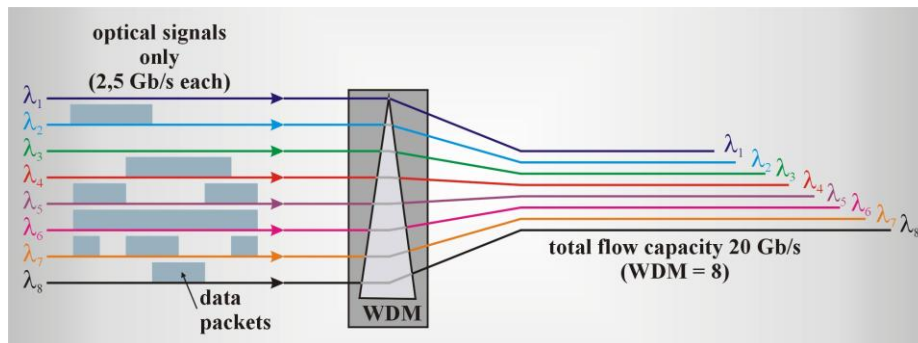


Fig. 7.62 Illustration of WDM technology

There are a variety of demultiplexer and multiplexer technologies to add or separate the channels including:

- Diffractive grating
- Laminar interfering filters
- Couplers
- Interferometers

Fig. 7.63 presents demultiplexer, in which selection of a wavelength is provided by applying diffraction gratings.

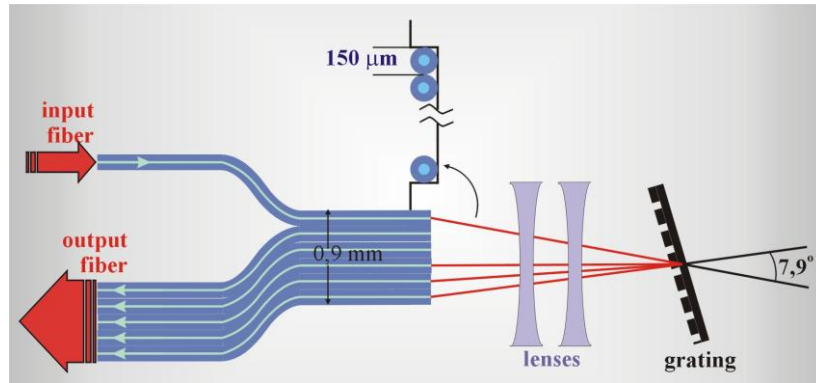


Fig. 7.63 Wavelength demultiplexer based on diffraction grating selection

The different wavelengths of light from the input fiber are focused on the diffraction grating. Each wavelength undergoes diffraction under different angle. Each of the diffracted beams corresponding to the different wavelengths is once again focused by the same focusing lens in the same focal plane, but at different places. These places correspond to the entrance to the output fibers where the beams of different wavelengths are introduced. Each beam corresponds to the different channel. The B bandwidth of a single channel depends on a fiber diameter  $D$  and the dispersion resolution of the grating  $\frac{dx}{d\lambda}$

$$B = \frac{d\lambda}{dx} D \quad (7.73)$$

For the I transmission window (850 nm) and a fiber of large core diameter on the order of 130  $\mu m$ , the typical bandwidth  $B$  is on the order of 20 nm, so the distance between the channels has to be larger than 20 nm.

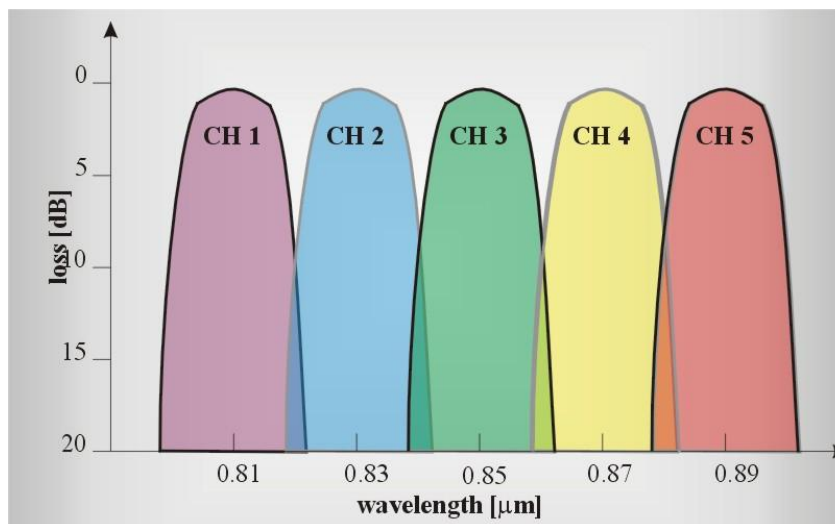


Fig. 7.64 The spectrum distribution of demultiplexer based on diffraction grating

The typical resolution of diffraction gratings in the II and III window are on the order of 1-2 nm and it is the bandwidth bottom limit. It is too large for WDM systems with a large number of channels in which distances between the channels are on the order of fractions of

nanometers. Therefore, the application of diffraction gratings is limited to systems with several channels.

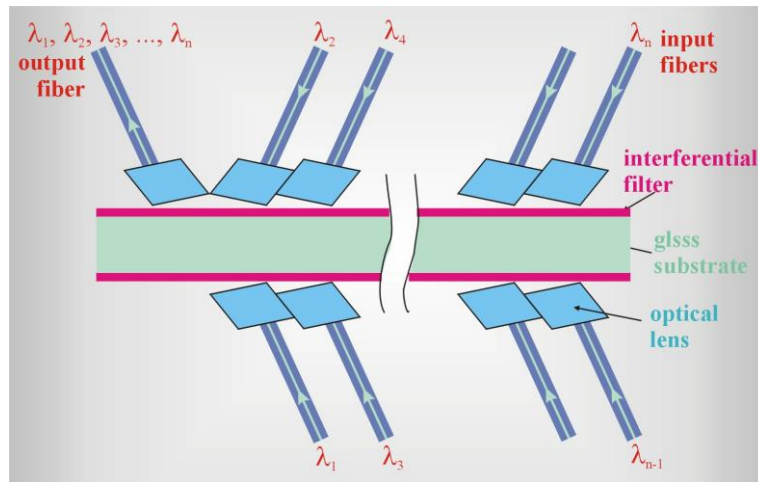


Fig. 7.65 Multiplexer based on interference filters

Another method of multiplexation is based on interference filters. Let us remind that interference filters are multilayer thin-film devices. They can be designed to function as an edge filter or bandpass filter. In either case, wavelength selection is based on the property of destructive light interference. This is the same principle underlying the operation of a Fabry-Perot interferometer. They consist of many thin dielectric layers of alternating, high and low values of refraction index, usually zinc sulfide and cryolite, each of which is a quarterwave thick, respectively. Together, the quarterwave coatings forming the reflective layer is called a stack. Incident light is passed through two coated reflecting surfaces. Fresnel reflection, which depends on difference of refraction indices, takes place at the interfaces. The distance between the reflective coatings determines which wavelengths destructively interfere and which wavelengths are in phase and will ultimately pass through the coatings. If the reflected beams are in phase, the light is passed through two reflective surfaces. If, on the other hand, the multiple reflections are not in phase, destructive interference reduces the transmission of these wavelengths through the device to near zero. In an interference filter, the gap between the reflecting surfaces is a thin film of dielectric material called a spacer. It has a thickness of one-half wave at the desired peak transmission wavelength. On either side of this gap are the two reflecting layers. The combination of two stacks and the spacer comprise a one cavity bandpass filter.

The next group of devices used as (de)multiplexers are couplers/splitters which were discussed in chapter 7.1.3. As we showed in chapter 7.1.3.1, couplers using the Bragg gratings can act both as switches and add /drop WDM (de)multiplexers (Fig. 7.66). The add / drop multiplexers are applied to change signal routing in order to propagate along different optical paths. The name - add and drop multiplexer defines its basic function – they add or remove some channels from a given optical path.

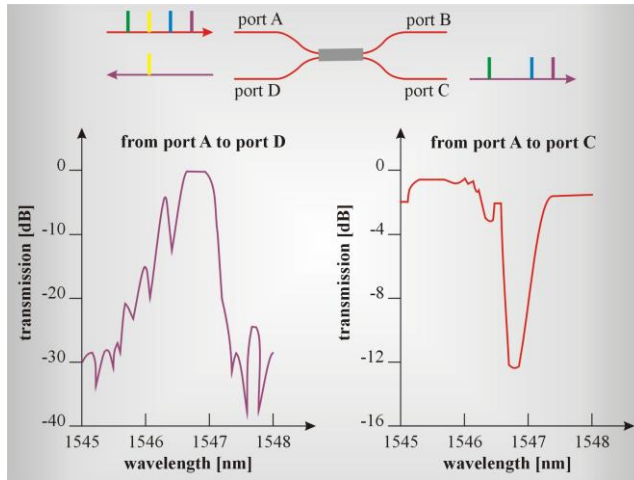


Fig. 7.66. Add/drop multiplexer. Adopted from Alcatel, Optical Networks Tutorial,

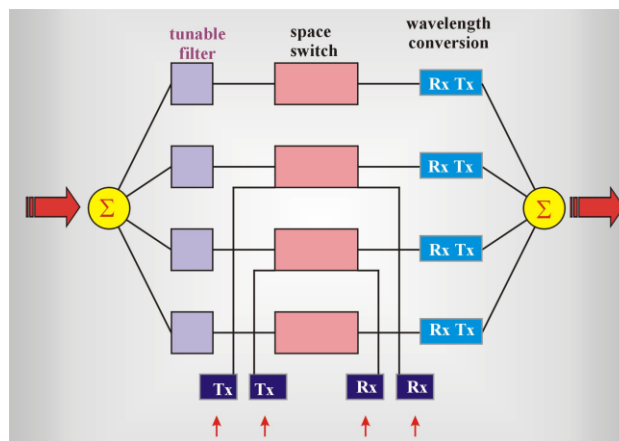


Fig. 7.67. Application of add/drop multiplexer. Adopted from Alcatel, Optical Networks Tutorial

The role of add/drop multiplexers can be played by interferometers. We can distinguish the following interferometers

- Fabry–Perot (FP)
- Sagnac (S)
- Mach- Zehnder (MZ)
- Michelson (M)

As we know the Fabry–Perot resonator is the most common configuration in lasers. The resonance cavity consists of two mirrors: HR (high reflector) totally reflecting light ( $R=100\%$ ), OC mirror partially transmitting the light (output coupler), active medium and pumping source. The standing wave is generated in resonance cavity when the condition is fulfilled

$$n \frac{\lambda}{2} = L \quad (7.74)$$

where  $n$  is the integer type number,  $L$  is the resonator length. The mirror in FP resonator can be replaced by the reflecting Bragg gratings.

The field intensity  $E(\vec{r}, t)$  inside the resonator is the sum of waves propagating forward and backward

$$E(\vec{r}, t) = \frac{1}{2} F(x, y) \{ A(z) \exp[i(\tilde{\beta}z - \omega t)] + \beta(z) \exp[-i(\tilde{\beta}z + \omega t)] \} + c.c \quad (7.75)$$

where  $F(x,y)$  is the transverse distribution,  $A(z)$  and  $\beta(z)$  are amplitudes of waves propagating along the direction  $\pm z$ . One can show [15] that

$$A(L) = \frac{(1 - R_m)A(0)}{1 - R_m \exp(i2L\tilde{\beta})} \quad (7.76)$$

where  $R_m$  is the reflection coefficient. Transmission  $T_R$  of FP resonator is expressed by formula [16]

$$T_R = \frac{P_K}{P_0} = \left| \frac{A(L)}{A(0)} \right|^2 = \frac{(1 - R_m)^2}{(1 - R_m)^2 + 4R_m \sin^2(\phi_R / 2)} \quad (7.77)$$

where  $P_K$  is an output power,  $P_0$  is an input power,  $\phi_R$  is a phase shifting after round-trip distance  $L_R = 2L$

$$\phi_R = \tilde{\beta}L_R \quad (7.78)$$

The phase shifting is caused by linear  $\phi_0$  and nonlinear effects  $\phi_{NL}$

$$\phi_R(\omega) = \phi_0(\omega) + \phi_{NL} = [\beta(\omega) + \Delta\beta_{NL}]L_R \quad (7.79)$$

When  $\phi_0 = 2\pi n$ , where  $n$  is an integer, and nonlinear effects are neglected,  $T_R = 1$  and it reaches the maximum.

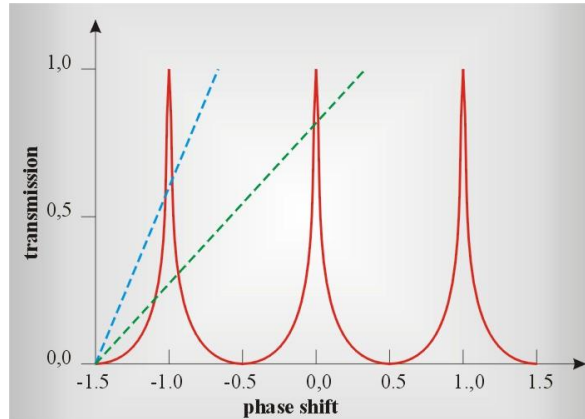


Fig.7.68. Transmission of FR resonator as a function of phase shift  $\phi_R = \phi_0$  (assuming that the non-linear effects are neglected)

Fig. 7.68. presents the transmission of FR resonator as a function of phase shift  $\phi_R = \phi_0$  assuming that the non-linear effects are neglected.

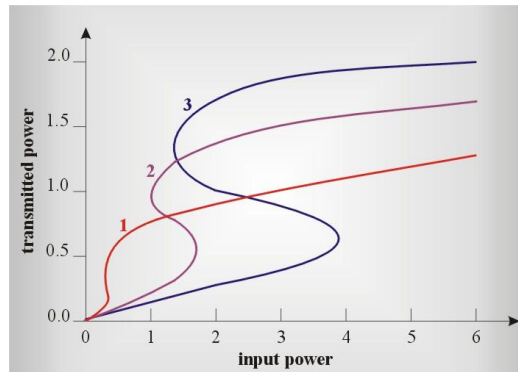


Fig. 7.69 Transmission in FT resonator, where the non-linear effects dominate ( $\phi_{NL} \neq 0$ ). Illustration of an optical bistability.

Figure 7.69 describes the transmission in FT resonator, where the non-linear effects dominate. The non-linear effects, caused by self-phase modulation SPM induce the additional shift of phase  $\phi_{NL}$  (eq.7.79), which depends on the input power. The most spectacular effect of nonlinearity in a resonator is the optical bistability [2,9].

The non-linear effects are widely used in interferometers, most often as optical switches. One of the most popular is Sagnac interferometer presented in Fig.7.70

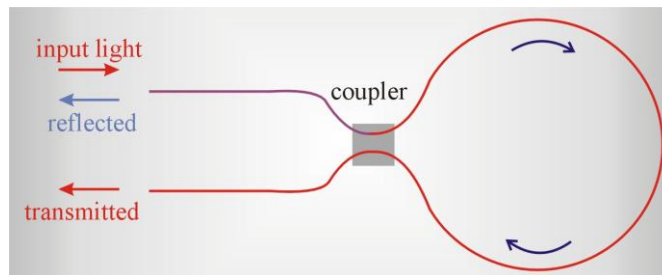


Fig. 7.70. Sagnac interferometer

The Sagnac interferometer consists of a loop of fiber linked with two ports of a coupler. Light enters through the entrance port 1, and is divided in a coupler into the wave propagating clockwise and the wave propagating counterclockwise. If we apply the coupler 50:50 (3 dB) and suppose that any non-linear phenomena do not occur in the fiber loop, the oppositely propagating waves do not generate any phase difference and both waves come back to port 1 as a reflected wave. There will be no signal in port 2. Also in the case when we introduce light of larger power and the non-linear phenomena in fiber loop begin to occur the phases difference is zero.

However, if the coupler separates the input beam into two oppositely propagating beams of different power, the non-linear effects, mainly self-phase modulation SPM, cause phase difference. The phase difference causes that a beam is not reflected to the entrance port 1, but it is transmitted by the port 2. This means that the Sagnac interferometer acts differently when it is propagating small powers, and differently - when powers are growing up. In the first case (low power, non-linear effects are neglected) the output signal is sent by the port 1, in the second case (high power, non-linear effects play a role) - by the port 2, so the Sagnac interferometer works as a switch.

Let us explain theoretical basis of this behaviour. From equations (7.23) derived for the couplers we can write for the waves propagating clockwise ( $A_1$ ) and counterclockwise ( $A_2$ )

$$A_1 = \sqrt{\rho} A_0 \quad A_2 = i\sqrt{1-\rho} A_0 \quad (7.80)$$

where  $\rho = \cos^2(\kappa L_c)$ ,  $L_c$  is a coupler length,  $\kappa_{21} = \kappa_e = \kappa$  for the symmetrical coupler. After full path in the loop of length L the waves meet in the coupler having modified phases

$$\begin{aligned} A_1 &= A_1 \exp\left[i\phi_0 + i\gamma(|A_1|^2 + 2|A_2|^2 L)\right] \\ A_2 &= A_2 \exp\left[i\phi_0 + i\gamma(|A_2|^2 + 2|A_1|^2 L)\right] \end{aligned} \quad (7.80)$$

where  $\phi_0 = \beta L$ .

Using once again equations (7.23) for the coupler (now with the reversed ports) we can write

$$\begin{pmatrix} A_t \\ A_r \end{pmatrix} = \begin{pmatrix} \sqrt{\rho} & i\sqrt{1-\rho} \\ i\sqrt{1-\rho} & \sqrt{\rho} \end{pmatrix} \begin{pmatrix} A_1 \\ A_2 \end{pmatrix} \quad (7.81)$$

where  $A_t$  is an amplitude of the transmitted wave (port 2),  $A_r$  is the amplitude of the reflected wave (port 1). Using (7.80) and (7.81) we can express the transmission T of the Sagnac interferometer as

$$T = \left| \frac{A_t}{A_0} \right|^2 = 1 - 2\rho(1-\rho)\{1 + \cos[(1-2\rho)\gamma P_0 L]\} \quad (7.82)$$

where  $P_0 = |A_0|^2$ . When  $\rho = 0.5$  (coupler 3 dB), the transmission T=0 and the beam comes back to the port 1 (100% reflection) both for low and high powers. When  $\rho \neq 0.5$ , the transmission T as a function of input power  $P_0$  is shown in Fig.7.71.

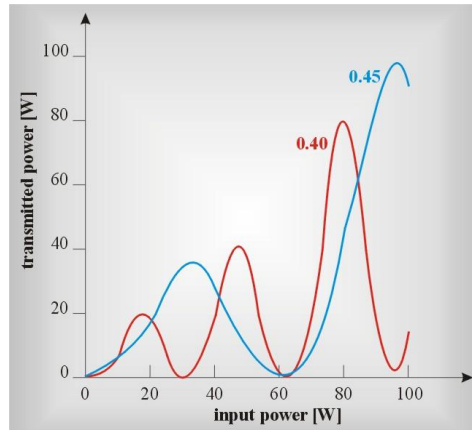


Fig. 7.71. Dependence of transmitted power as a function of input optical power

As we can see, for small powers small fraction of light is transmitted  $\{T \approx 1 - 4\rho(1-\rho)\}$ . For large powers the transmission is about 100% ( $T \approx 1$ ) when

$$|1 - 2\rho|\gamma P_0 L = (2m - 1)\pi \quad (7.83)$$

In practice only the first peak is used ( $m = 1$ ). We can estimate the input power  $P_0$ , which allows the Sagnac interferometer to act as a switch from formula (7.83). Let take the



typical values of  $\gamma = 10W^{-1}$ ,  $L = 100m$ ,  $\rho = 0.45$ , and we get  $P_0 \approx 30W$ . It indicates that the switching threshold is quite high. To reduce the switching threshold we can introduce asymmetry to Sagnac interferometer. One of them is placing a fiber amplifier just after the coupler. Then even the 3dB coupler shows asymmetry because beams propagating in opposite directions are not identical. Indeed, the beam propagating clockwise is amplified at the beginning of the loop, while the counter-clock propagating wave - at the end. Both beams have different intensities after amplification, so the non-linear effect of self-phase modulation causes different phase shift  $\phi_{NL}$ . Another way of increasing the non-linearity of the interferometer loop is introduction to loop the non-linear element in the form of semiconductor amplifier. It leads to the significant reduction of the loop length to 1m. For comparison, the nonlinearity of a fiber caused by the crossing phase modulation XPM is very small and in order to generate the suitable phase difference  $\Delta\phi_{NL}$  the loop length should be on the order of 10 km. Disadvantage of semi-conductor amplifier is a quite long response time  $\sim 1ns$ , which limit the applications in telecommunication to systems with bit rates smaller than Gb/s. However, the slow response time can be omitted by a simple trick. Semi-conduction amplifier is placed asymmetrically in a fiber loop by shifting from the loop centre. Thus, slow response time does not play any role, because the on/off time is determined by the shift from the centre. Such a device can work even in terahertz systems (TOAD, terahertz optical asymmetric demultiplexer).

So far we presented the Sagnac interferometer based on non-linear effect of self-phase modulation SPM. It is also possible to use cross phase modulation XPM. To obtain this effect one should introduce the control signal (sometimes called a pumping signal or a clock signal) to the interferometer loop. The control signal propagates in the same direction as one of the beams and opposite to the second one. The non-linear shift of phase  $\phi_{NL}$  generated by the cross-phase modulation takes place only for one of these beams. The cross phase modulation XPM is often applied in OTDM demultiplexing (optical time division multiplexing). Fig. 7.72 illustrates the way of demultiplexing with Sagnac interferometer and the cross phase modulation XPM [17].

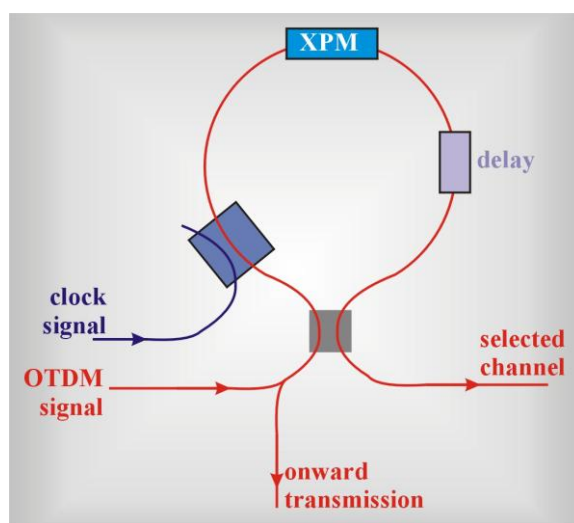


Fig. 7.72 Demultiplexing in Sagnac interferometer with the cross phase modulation.



The control pulse (optical clock) consists of a series of optical pulses at velocities expressed by number bits per second. The control pulse propagates clockwise or counterclockwise. The OTDM signal enters the coupler and is split into two beams propagating in opposite directions. The clock pulse is synchronized in time with the pulses of only one channel (1) from the OTDM stream. So, only signals of channel (1) overlap with the clock signals. The XPM interactions between the control signal and the two oppositely propagating beams generates the phase difference  $\phi_{NL}$ . When power of the control pulse and the length of the loop L are chosen in such a way that  $\Delta\phi_{NL} = \pi$  for a chosen channel (1), only the signal (1) is further transmitted, the signals of the other channels are reflected in the entrance port. Using this method one can select different channels, delaying the control pulse to synchronize it with a given channel.

Another type of interferometer applied in telecommunication as demultiplexer, switch or modulator is Mach-Zehnder (MZ) interferometer. We have already considered its application as a modulator. Now let consider now MZ as add/drop multiplexer. Fig. 7.73 presents MZ interferometer used as a add/drop multiplexer (filter) applied in WDM technologies.

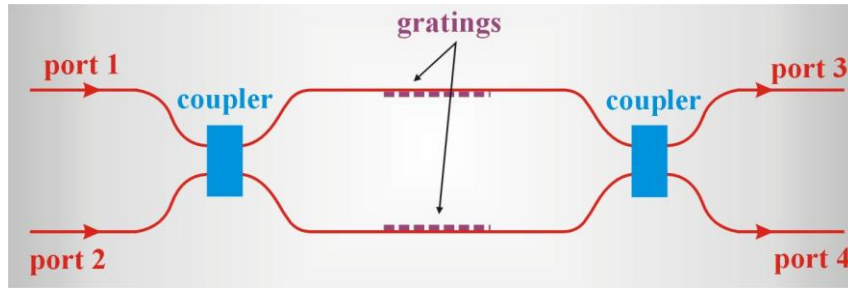


Fig. 7.73 MZ interferometer used as add/drop multiplexer (filter) applied in WDM technologies.

The operation principle of MZ is the same as for the Sagnac interferometer. The only difference in configuration is that the loop is replaced by two branches. The asymmetry that creates non-linear phase can be introduced in many ways (length, non - linear element). In contrast to Sagnac interferometer there is no reflected light coming back by the entrance port 1.

The theory of operation principle of MZ interferometer as a non- linear switch or a add/drop multiplexer is very similar to that presented for Sagnac interferometer. Let the continuous wave at power  $P_0$  enter by the port 1. At the entrance to the second coupler we have

$$A_1 = \sqrt{\rho_1} A_0 \exp\left[i\beta_1 L_1 + i\rho_1 \gamma |A_0|^2 L_1\right] \quad (7.84)$$

$$A_2 = i\sqrt{1 - \rho_1} A_0 \exp\left[i\beta_2 L_2 + i(1 - \rho_1) \gamma |A_0|^2 L_2\right]$$

where  $\beta_1$  and  $\beta_2$  are the propagation constant,  $L_1$  and  $L_2$  are the side lengths of MZ interferometer. The output power from the ports 3 and 4 can be calculated from the transformation matrix

$$\begin{pmatrix} A_3 \\ A_4 \end{pmatrix} = \begin{pmatrix} \sqrt{\rho_2} & i\sqrt{1 - \rho_2} \\ i\sqrt{1 - \rho_2} & \sqrt{\rho_2} \end{pmatrix} \begin{pmatrix} A_1 \\ A_2 \end{pmatrix} \quad (7.85)$$

The fraction of power transmitted through the port 3  $T_3 = |A_3|^2 / |A_0|^2$  is

$$T_3 = \rho_1 \rho_2 + (1 - \rho_1)(1 - \rho_2) - 2[\rho_1 \rho_2 (1 - \rho_1)(1 - \rho_2)]^{1/2} \cos(\phi_L + \phi_{NL}) \quad (7.86)$$

where the term  $\phi_L$  represents the linear contribution to the phase shift

$$\phi_L = \beta_1 L_1 - \beta_2 L_2 \quad (7.87)$$

and  $\phi_{NL}$  represents the non-linear contribution to the phase shift:

$$\phi_{NL} = \gamma P_0 [\rho_1 L_1 - (1 - \rho_1) L_2] \quad (7.88)$$

When  $\rho_1 = \rho_2 = \frac{1}{2}$  and  $L_1 = L_2$ , the interferometer becomes a symmetrical interferometer consisting of two couplers 3dB (50 : 50). The transmission  $T_3$  gets much simpler form

$$T_3 = \sin^2(\phi_L / 2) \quad (7.89)$$

where only the linear effects contribute to the shift of phase. Because a phase shift  $\phi_L$  depends on frequency, therefore the MZ interferometer in the linear version operates as an optical filter.

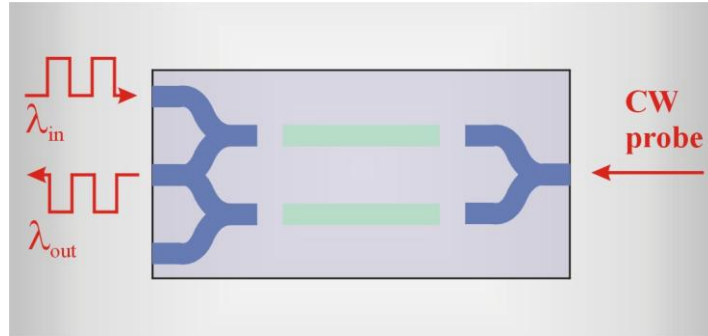


Fig.7.74. MZ interferometer in the linear version operates as an optical filter

### 7.2.6. Switches

Both in traditional copper based technology and in optical transmission signals must be directed to the recipients (Fig. 7.75). The traditional switches used in optical transmission are electro-optical devices. They do not require quick switching which means that the devices that switch light can usually stay at the same position for a relatively long time, let say tens of milliseconds. However, with development of dynamic routing, the need of quick switching becomes very important. That is why the nowadays optical switches are entirely optical devices.

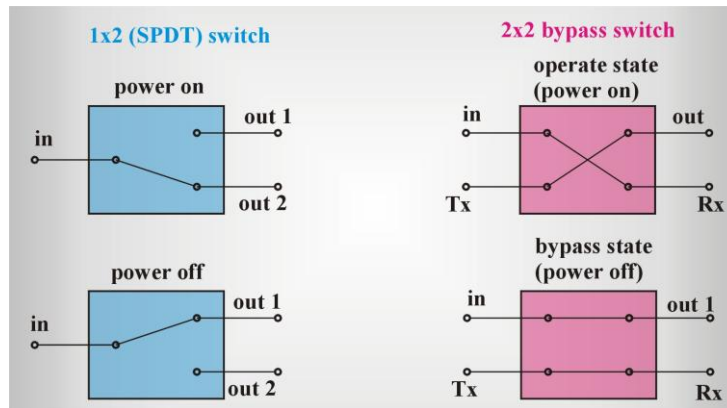


Fig. 7.75 Typical configurations of switches

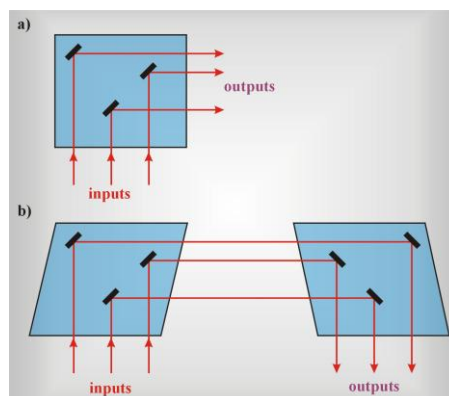
Optical switches can be classified according to their physical properties as

- thermo-optical
- electro-optical
- opto-mechanical
- microelectromechanical MEMS (ang. micromechanical systems)
- acoustical
- entirely optical switches, based on the non - linear optical phenomena.

**Thermo-optical switches** operate on polymer or silica waveguides. Their operation work is based on change of refraction index with temperature. Thermo-optical switches are slow and cannot be applied in large rate systems.

**Electro-optical switches** are based on semi-conductor technology and their operation work is based on change of refraction index with electric field. Some types of Mach – Zehnder interferometer use electro-optical effects.

However, both electro-optic and thermo-optical switches have large losses, large reflection, and stability smaller than the opto-mechanical switches. On the other side, **opto-mechanical switches** are slow, their response time is on the order of 10-100 ms. They belong to the oldest switches, where switching is achieved by using stepped motors to direct light in a proper place. Their large sizes has been reduced in a new generation of switches – MEMS microelectromechanical switches (Fig. 7.76).



Rys. 7.76. MEMS microelectromechanical switch, a) two-dimensional 2D, b) three-dimensional 3D

2D MEMS switches consist of mirrors placed in cross-shaped configurations. Each of them can be in one of two states: ON - reflection, OFF - transmission. The switch with  $N \times N$  ports requires  $N^2$  mirrors. The 3D MEMS switch consists of  $N$  or  $2N$  mirrors. Mirrors can rotate around two axis. The MEMS switches are the matrix of micro mirrors of size on the order of 5  $\mu\text{m}$ , hanged on elastic semi-conductor holders steered by electromagnetic field. This device is an optomechanical switch and change of mirror positioning requires time.

Fig. 7.77 presents solution used by Lucent WaveStar LambdaRouter.

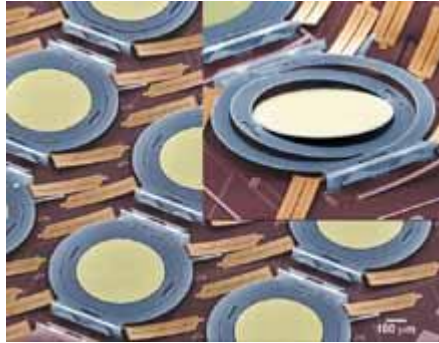


Fig. 7.77 The MEMS switch of Lucent WaveStar LambdaRouter company. <http://www.chip.pl/images/0099> Alcatel, Optical Networks Tutorial

The entirely optical switches are based on non-linear optical phenomena. The most often used switches are Sagnac interferometer and Mach-Zehnder interferometer .

1. A.W. Snyder, J. Opt. Soc. Am. 62, 1267 (1972), A.Snyder, J.Opt. Soc. Am., 63, 1518 (1973), A.W. Snyder, J.D. Love, Optical Waveguide Theory, Chapman and Hall, London, 1983
2. G.P. Agrawal, Nonlinear Fiber Optics, Academic Press 2001
3. R. Tewaei, K. Thyagarajan, J. Lightwave Technol. 4, 386 (1986)
4. S.M. Jeneon, IEEE J. Quantum Elektron. QE-18, 1580 (1992)
5. H. Abramczyk, Introduction to laser spectroscopy, Elsevier, 2005
6. W. Koechner, Solid-State Laser Engineering, 5<sup>th</sup> Edition, vol. 1, Springer-Verlag (1999)
7. L.M. Frantz, J.S Nodvik, J. Appl. Phys. 34 (1963) 2346
8. R. Bellman, G. Birnbaum, W.G. Wagner, J. Appl. Phys. 34 (1963) 780
9. G.P. Agrawal, Applications of Nonlinear Fiber Optics, Academic Press, 2001
10. M.N. Islam, Raman amplifiers for telecommunications, IEEE Journal of Selected Topics in Quantum Electronics, Vol. 8, no.3, 2002
11. R.H. Stolen, E.O. Ippen, Raman gain in glass optical waveguides, Appl. Phys. Lett., vol. 22, no.6, 1973
12. R.O`B. Carpenter, J. Opt. Soc. Am. 40 (1950) 225

13. B. Ziętek, Optoelektronika, Wydawnictwo Uniwersytetu Mikołaja Kopernika, 2005
  14. J. Wilson, J.F. Hawkes, Optoelectronics - an introduction, Prentice Hall, New York, 1989
  15. O. Svlto, Principles of Lasers, 4<sup>th</sup> edition, Plenum Press, New York, 1998
  16. M. Born, F. Wolf, Principles of Optics, 7<sup>th</sup> edition, Cambridge University Press, New York, 1999, ch.7
  17. P.A. Adrekson, N.A. Olsson, J.R. Simpson, D.J. Digiovanni, P.A. Morton, T.Tanbun-  
Ek, R.A. Logan, K.W. Wecht, IEEE Photon Technol. Lett. 4, 644 (1992)
-